

Comparative Study of Different Probing Techniques for the Analysis of the Free Volume Distribution in Amorphous Glassy Perfluoropolymers

Johannes C. Jansen,^{*,†} Marialuigia Macchione,^{†,‡} Elena Tocci,[†] Luana De Lorenzo,[†] Yuri P. Yampolskii,[§] Olga Sanfirova,[§] Victor P. Shantarovich,^{||} Matthias Heuchel,[⊥] Dieter Hofmann,[⊥] and Enrico Drioli[†]

[†]Institute on Membrane Technology, ITM-CNR, Via P. Bucci 17/C, 87030 Rende (CS), Italy, [‡]Department of Chemistry, University of Calabria, Via P. Bucci 14/D, 87030 Rende (CS), Italy, [§]A.V. Topchiev Institute of Petrochemical Synthesis, 29 Leninsky Prospect, 119991, Moscow, Russian Federation, ^{||}N. N. Semenov Institute of Chemical Physics, Russian Academy of Sciences, 4 Kosyginova Str., 117334, Moscow, and [⊥]GKSS Research Center, Institute of Chemistry, Kantstrasse 55, D-14513, Teltow, Germany

Received June 10, 2009; Revised Manuscript Received August 14, 2009

ABSTRACT: A comparative study of five different experimental and computational methods is presented for the characterization of the overall free volume (FV) and the free volume element (FVE) size and shape distribution in amorphous glassy perfluoropolymers (PFPs). Experimental results from the photochromic probe (PCP) method, positron annihilation lifetime spectroscopy (PALS), and inverse gas chromatography (IGC) were confronted with literature data from ¹²⁹Xe NMR spectroscopy, and the experimental data were further compared with molecular dynamics (MD) simulations and a combination of MD studies and the well-known Bondi method as well as a modified Bondi method. An evaluation of the advantages and the limits of each method is presented. This is the first reported study on a so vast number of complementary techniques applied on a single glassy polymer, in this case Hyflon AD perfluoropolymer, and is also the first successful application of the photochromic probe technique in such materials. In two different grades of Hyflon AD, the polymer with the highest content of the stiff cyclic comonomer was found to have a slightly larger average FVE size but a lower void concentration, explaining the nearly identical density and fractional free volume (FFV) of the two samples. PALS furthermore demonstrated a similar trend for solution-cast samples in comparison with melt-pressed samples, the latter having FVEs with a smaller size but a higher concentration. The data from IGC seem to correspond most closely to those of the PCP method. Differences between the results from the individual techniques derive mainly from the fundamentally diverse nature of the various probing methods but also from the different capacity to take into account the FVE shape. Only MD simulation studies, using detailed atomistic packing models, can give such deep insight into the spatial arrangement of the FVEs directly. Besides giving the highest level of detail, MD simulations can thus help to understand the possible limits of the experimental methods. Knowledge of their free volume distribution is of fundamental importance to gain more insight into the mass transport phenomena in these materials, relevant for their successful application in the emerging field of synthetic membranes for gas and vapor separations.

1. Introduction

1.1. Free Volume in Polymers. The search for novel polymeric materials with desired combinations of gas permeability and permselectivity to separate gas mixtures is an important challenge in membrane science. Glassy polymers are often the most useful materials for gas separation membranes because of their superior permeability/selectivity balance. Polymeric glasses are in a nonequilibrium state¹ with a continuous evolution toward equilibrium through spontaneous, but usually very slow, molecular rearrangements at temperatures far below the glass transition temperature, T_g . Since macroscopic properties of glassy polymers depend on their inefficiency of packing or free volume,^{2,3} a rational determination of the relationship between chemical structure and transport parameters, such as permeability and diffusion coefficients, becomes important.

The concept that free volume in polymer glasses is composed of local free volume elements of different sizes has a

broad theoretical support.^{1–4} Only recently more experimental data on the distribution of local free volume are gradually becoming available. Various studies have demonstrated a direct correlation between free volume and gas transport in polymeric membranes.^{5,6} Variations of free volume due to physical aging³ may lead to dramatic changes in the gas permeability, for instance, for poly[1-(trimethylsilyl)-1-propyne] (PTMSP), for which the permeability decreases more than 2 orders of magnitude in only 100 days.⁷ This behavior depends strongly on the nature of the polymer because another high free volume polymer, Teflon AF, is reported to be highly stable toward physical aging.⁸

Free volume in polymers can be determined by numerous methods,^{9,10} such as positron annihilation lifetime spectroscopy (PALS),^{11,12} inverse gas chromatography (IGC),¹³ and ¹²⁹Xe NMR spectroscopy,¹⁴ and by electrochromic,¹⁵ spin probe,¹⁵ or photochromic probe methods.¹⁶

Data on high free volume perfluorinated polymers are rather rare.^{17–19} For Hyflon AD polymers only the total void fraction estimated by the group contribution method²⁰ and the average void size determined by ¹²⁹Xe

*Corresponding author: Tel +39 0984-492031, Fax +39 0984-402103, e-mail johannescarolus.jansen@cnr.it.

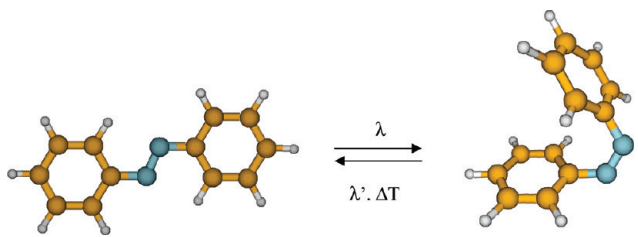


Figure 1. Photochemical isomerization of *trans*-azobenzene. The reverse reaction can be induced thermally or by irradiation with light of a distinct wavelength.

NMR spectroscopy¹⁴ have been published in the literature. The calculated fractional free volume of Hyflon AD60X and Hyflon AD80X of about 23% (Supporting Information) poses these polymers near other high FFV polymers such as Teflon AF 2400 and Teflon AF1600²¹ and clarifies the reason for the high permeability of these polymers, significantly above those of most conventional glassy polymers^{22,23} like for instance polysulfone and other polymers commonly used in commercial gas separation membranes, with FFVs ranging from around 12–17%.

1.2. Photochromic Probing. Photochromism of molecular probes is a phenomenon which is sensitive to the distribution of local free volume in polymer glasses.¹⁶ Photochromic molecular probes in glassy polymers were first used by Gardlund.²⁴ Since then, they have been successfully used in evaluating the free volume distribution of various matrices, including polycarbonate,^{25,26} polystyrene,^{16,27} poly(vinyl acetate),²⁶ poly(methyl methacrylate),²⁸ epoxy resin,^{29,30} and other polymers.³¹ For this purpose, photochromic or photoisomerizable molecules, usually stilbenes and azobenzenes, are dispersed homogeneously within the polymer matrix. Upon irradiation with UV or visible light with the proper wavelength and/or upon heating, the photochromic molecules may undergo *trans*–*cis* isomerization and the reverse reaction (Figure 1). In the case of azobenzenes this isomerization involves a rotation around the double bond and the swapping of one of the phenyl groups from one side to the other. In solution the extent of the reaction from the more stable *trans*-isomer to the *cis*-isomer depends on the probe structure and on the experimental conditions, such as wavelength, light intensity, irradiation time, and the solvent polarity, but much less on its viscosity.³² Probe isomerization is dramatically slowed down in a glassy polymer matrix, and depending on the specific probe size and volume, also the extent of isomerization is usually lower. Nevertheless, even in glassy polymers the isomerization can be accelerated by creation of a local rubbery environment.³³ This principle can be used for sensing glass transitions in polymeric materials.^{34,35}

The difference between the rate and especially the extent of probe isomerization in solution and in a glassy polymer matrix forms actually the basic principle of the photochromic probe method for free volume analysis, originally developed by Victor and Torkelson¹⁶ and used in the present paper.

The crucial hypothesis, at the basis of the photochromic probe technique, is that photoisomerization in the glassy state requires a minimum critical size of local free volume in the vicinity of the chromophore. The isomerization requires a certain amount of extra volume during the rotation of the molecule from the *trans*- to *cis*-configuration¹⁶ not only because the molecular volume of the *cis* and the *trans* isomers may be different but also because the rotation itself requires some freedom of motion. This is schematically displayed in

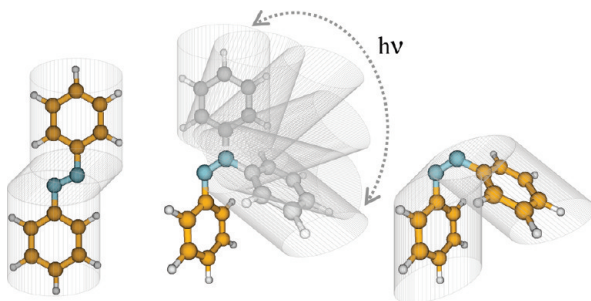


Figure 2. Schematic representation of the volume occupied by an azobenzene probe molecule in the *trans*-form (left) and in the *cis*-form (right) and of the extra volume required for the photoinduced *cis*–*trans* isomerization reaction (center).

Figure 2. If this volume is available, i.e., if the photochromic molecule is located in a sufficiently large free volume element, then photoisomerization will occur; otherwise it will not. This procedure thus allows the qualitative determination of the free volume distribution if a series of photochromic molecules is used which require each a different volume for the *trans*–*cis* isomerization reaction. An important and generally accepted assumption is that the dye molecule does not influence the free volume itself and that it does not interact with the polymer matrix. Furthermore, the polymer chain dynamics must be sufficiently slow that there is no significant relaxation of the free volume elements on the time scale required to realize the *trans*–*cis* transition. In practice, the amount of probe photoisomerization in a glassy polymer relative to that in dilute solution in a nonviscous model solvent, where free volume is not a constraint to isomerization, is measured as a function of the volume required for photoisomerization of the probe.

The advantage of the photochromic probe method for free volume determination is the relative simplicity of the experimental procedures and of the equipment required, in contrast to for instance PALS and NMR analysis. However, a critical factor is the knowledge of the volume required for the isomerization reaction. This is usually not known, but it can be estimated on the basis of the van der Waals volume of the probe molecule and on geometric considerations to calculate the volume swept during the isomerization reaction.¹⁶ Furthermore, the method is based on several important assumptions, for instance, that the probe molecules are homogeneously distributed in the polymer matrix, that no clustering occurs, and, most important, that they do not influence the polymer matrix or vice versa.

Since it is difficult to check the validity of some of the above assumptions and the fulfillment of these conditions, a comparison with the results of other probe methods is highly desirable. In the present work the PCP method is compared with results of IGC and PALS analysis, MD simulations, and literature data from ¹²⁹Xe NMR spectroscopy.

1.3. Positron Annihilation Lifetime Spectroscopy. Among the probe methods to study free volume in polymers, positron annihilation lifetime spectroscopy (PALS) has found the widest application and is considered as the most developed and reliable technique.^{9,10,36} This method is based on the measurement of the lifetimes of positrons before annihilation in polymers. The most commonly used source that emits positrons is the radioactive ²²Na isotope. The emitted positrons, when getting into condensed matter (polymer), can exist in the form of free positrons (e^+) and hydrogen-like positronium atoms (Ps), combinations of positron and electron, until their annihilation. Depending of the spin of this

species, they can form p-Ps (antiparallel spins of e^+ and e^-) and o-Ps (parallel spins). Intramolecular annihilation of p-Ps and annihilation of free positrons proceed with high rate, and we shall not discuss them in this paper, since we use the PALS method. Annihilation in the form of o-Ps is characterized by much longer lifetimes. In vacuum the intrinsic lifetime of this bound state is 142 ns. However, in condensed matter the lifetimes are shortened, usually by 2 orders of magnitude, due to coupling of wave functions of o-Ps and electrons of the atoms of the material that surround o-Ps. In conventional glassy polymers they are in the range of 1.5–3.0 ns.^{37–39} The paradigm of the PALS method is that o-Ps in polymers will move into the regions with reduced density, the free volume elements (FVE), where they will then survive until their annihilation. The principle of the PALS method for free volume evaluation is that the annihilation is slower the larger the size of the FVE is. The mathematical expression of this statement is the semiempirical equation, originally proposed by Tao⁴⁰ for a spherical potential well (spherical pore) and later used by several other authors [e.g., refs 41 and 42]:

$$\tau_3 = \frac{1}{2} \left[1 - \left(\frac{R_i}{R_0} \right) + \frac{1}{2\pi} \sin \left(\frac{2\pi R_i}{R_0} \right) \right]^{-1} \quad (1)$$

where τ_3 is o-Ps lifetime, R_i is the corresponding radius of a spherical FVE, and $R_0 = R + \Delta R$ (where the adjustable parameter ΔR is usually fixed at 1.66 Å⁴²).

The shape of the pore can be also approximated by a channel (cuboid or cylinder), which give results very close to each other for the same width and length,^{39,43} or by a slit. For the cuboid case, the dependence of τ_3 on the cuboid parameters (sides) α_1 , α_2 , and α_3 is given by the equation⁴³

$$\tau_3 \approx 0.5 \left[1 - \prod_{i=1}^3 \left(\frac{\alpha_i}{\alpha_i + 2\Delta R} + \frac{1}{\pi} \sin \frac{\pi \alpha_i}{\alpha_i + 2\Delta R} \right) \right]^{-1} \quad (2)$$

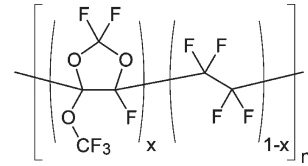
where ΔR has the same meaning as in eq 1.

For the same lifetime τ_3 , channel or slit geometry gives smaller pore width. The effect saturates with pore or slit length.³⁹

It is known that dissolved oxygen in polymers can quench o-Ps in the pores or FVEs of a polymer, thus reducing their lifetimes.^{44,45} This effect is important only for high free volume polymers and virtually disappears for the polymers having smaller sizes of free volume elements.⁴⁶ Since the Hyflons used in the present work exhibit relatively high gas permeability, the measurements were carried out in the atmosphere of nitrogen.

1.4. Inverse Gas Chromatography. Inverse gas chromatography (IGC) is a dynamic method for investigation of the thermodynamic properties of polymers.⁴⁷ Traditionally, it has been applied for the investigation of polymers above their glass transition temperature. However, studies of polymers with large free volume and high gas permeability showed that it is applicable also for glassy polymers.^{6,7,10} In such polymers diffusion limitations do not prevent establishing sorption equilibrium, so such characteristics as activity coefficients and the parameters of their temperature dependence $\bar{H}_1^{E,\infty}$ and $\bar{S}_1^{E,\infty}$ can be found. It was shown that for series of solutes with widely varying sizes the dependence of $\bar{H}_1^{E,\infty}$ passes through a minimum when the molecular mass of solutes or their size changes significantly. It was first assumed¹⁰ and later confirmed using different polymers as examples⁶ that the coordinates of these minima can be

Scheme 1. Chemical Structure of Hyflon AD60X ($x = 0.6$) and Hyflon AD80X ($x = 0.8$)



interpreted as an average size of free volume in the polymers. In these studies, the *n*-alkane series C₃–C₁₃ was used as molecular probes. Critical volume V_c or molecular volume at boiling point V_b can be used as a measure of the size of the probe and, hence, of the free volume element (FVE) size. The coordinates of these minima ($V_{c(\min)}$) correlate with the gas permeability of different polymers studied using IGC, while the obtained FVE sizes are in a reasonable agreement with the results of other probe methods (see e.g. ref 11). All this served us an incentive to use also this method for the investigation of the free volume in Hyflon AD samples.

1.5. Molecular Dynamics Simulations. With the development of extremely powerful computer hardware and software in the past few decades, computational methods have become an important source of information on the chemical–physical properties of polymers, allowing for instance the analysis of their free volume and transport properties.⁴⁸ In spite of the advances already made, the development of ever better force fields, calculation algorithms, and computer hardware remains a continuous challenge. Nowadays, several well-established simulation methods exist for the preparation of atomistic packing models, also for high free volume polymers, like PTMSP and Teflon AF, or for polymers containing strongly polar moieties, such as polyimides. Such simulated models allow an accurate determination of geometrical quantities, characterizing the three-dimensional structure and chain packing, and represent therefore a valid additional approach to study free volume properties of polymer materials.^{49–51}

1.6. Scope. The aim of the present work is to make a comparison between the most commonly used experimental probing techniques (PALS, IGC, ¹²⁹Xe NMR) and photochromic probing for the evaluation of the local free volume and the free volume element size and shape distribution in Hyflon AD glassy perfluoropolymers. Hyflon AD polymers are amorphous perfluorinated copolymers of tetrafluoroethylene (TFE) and 2,2,4-trifluoro-5-trifluoromethoxy-1,3-dioxole (TTD) (Scheme 1). These polymers have a high thermal, chemical, aging, weathering, and solvent resistance which is characteristic for perfluoropolymers (PFPs), like for instance polytetrafluoroethylene (PTFE). In contrast to the semicrystalline PTFE, Hyflon AD polymers are amorphous glasses with a modestly high T_g , as a result of the bulky TTD units in the polymer chain. Amorphous glassy PFPs of the Hyflon AD and the Teflon AF family are known for their relatively high FFV¹⁷ or void fraction, which is the reason for their high gas permeability.^{18,20} In the present work two different grades of Hyflon AD with different copolymer compositions are used.

2. Experimental Section

2.1. Materials. Hyflon AD60X was purchased from Solvay Solexis, and Hyflon AD80X was a free gift from the same company. These polymers (Scheme 1) have glass transition temperatures of 130 °C⁵² and 134 °C,²¹ respectively. In this study 1-methoxynonafluorobutane (3M, trade name HFE 7100, bp 60 °C, MW 250 g/mol) was used without further purification

Table 1. Structure of the Azobenzene and Stilbene Derivatives Used as Molecular Probes in the Present Studies

Probe molecules	Azobenzene derivatives		Stilbene derivatives	
	R	R'	X	Y
Azobenzene	H	H	-	-
Disperse orange 3	NO ₂	NH ₂	-	-
Disperse red 1	NO ₂	N(CH ₂ CH ₃)CH ₂ CH ₂ OH	-	-
Disperse orange 25	NO ₂	N(C ₂ H ₅)CH ₂ CH ₂ CN	-	-
Stilbene	-	-	H	H
4,4'-dinitrostilbene	-	-	NO ₂	NO ₂

as the solvent to prepare solution-cast films. Photochromic molecules were purchased from Aldrich and were used without further purification. Table 1 shows the chemical structure of the molecular probes used in this study. Dichloromethane (DCM) (Carlo Erba Reagenti, Italy) served as the solvent to prepare a concentrated mother solution of the photochromic molecules and was used as received.

2.2. Polymer Solubility Tests. Hyflon AD is completely soluble in the solvent HFE 7100. Cloud point measurements were carried out by dropwise addition of DCM to the polymer solution according to the method described in ref 53 in order to determine the maximum amount of DCM in the polymer solution without inducing phase separation. The maximum concentration of DCM in the polymer solution during membrane preparation was kept far below this upper limit.

2.3. Membrane Preparation. Pure dense Hyflon AD films were prepared by the controlled solvent evaporation method from a 5 wt % polymer solution in 1-methoxynonafluorobutane (HFE7100) as the solvent, cast in a Petri dish or in a metal ring, and placed on a glass plate. The films were first dried for at least 48 h at room temperature and ambient pressure, and after releasing from the glass plate with the aid of some water, they were further dried in a vacuum oven at 50 °C for 16–20 h.

The corresponding films doped with photochromic probes were prepared by an analogous procedure. Mother solutions of six different photochromic molecules in their most stable trans isomer were prepared separately at a concentration of 5.9 × 10⁻³ M in DCM. The dye solutions (1.5 wt % of the final solution mass) were added under rapid stirring to a 5 wt % Hyflon AD solution in HFE7100. Further film casting and membrane drying was identical to the standard procedure. The final dye concentration was 1.7 × 10⁻⁶ mol/cm³ in the polymer. In every step the solutions and films were covered by aluminum foil to protect them from exposure to light and to avoid uncontrolled photoisomerization reactions. The photochromic films were first dried for at least 48 h at room temperature and then in a vacuum oven at 50 °C for 6 h.

2.4. Photoisomerization and UV-vis Characterization. Photo-irradiation of the membranes was performed with a medium pressure mercury UV lamp (GRE 500W, Helios Italquartz). The proper wavelengths were selected by means of band-pass filters (OptoSigma). The trans–cis isomerization reaction of all chromophores was realized by means irradiating at 350 nm, using a quartz filter, and the back-reaction was induced by irradiation at 440 nm, using a blue glass filter. Studies of the kinetics of the trans–cis photoisomerization recommended an irradiation time of 15 min to have the maximum of photoconversion for all types of dye; the lamp to film distance was 15 cm. Band pass filters were placed directly onto the sample surface to avoid irradiation of the films by unfiltered scattered light from the sides, which may compromise the efficiency of the photoisomerization.

The molar absorption coefficients, $\varepsilon_{\text{trans}}$ and ε_{cis} , of photochromic molecules dispersed in a 70/30 w/w mixture of HFE 7100 and DCM at a concentration of 5.93 × 10⁻³ mol/L, were calculated by absorbance measurements, using the Lambert–Beer law:

$$A = Ced \quad (3)$$

where A is the value of the absorbance peak at the maximum absorption wavelength, λ , of the dye, C is the concentration, and d is the path length of the UV beam in the cuvette containing the solution. Results are listed in Table I of the Supporting Information. The photochromic solutions were prepared and stored in aluminum foil-wrapped flasks to avoid accidental light exposure leading to uncontrolled photoisomerization. All absorbance measurements were carried out at ambient temperature. The spectrophotometric analysis was performed on a UV–vis spectrophotometer (model Shimadzu UV 1601) interfaced to a PC for the data elaboration. The resulting cis fraction or degree of trans–cis isomerization in the films, Y , was calculated from the following equation:

$$Y = \frac{1 - A/A_{\text{dark}}}{1 - \varepsilon_{\text{cis}}/\varepsilon_{\text{trans}}} \quad (4)$$

where A_{dark} is the initial peak absorbance with only trans isomer present, A is the actual peak absorbance, and ε_{cis} and $\varepsilon_{\text{trans}}$ are the molar absorption coefficients of the cis and trans isomers, respectively. The maximum isomerization in dilute solution is considered as a reference (100%) for the calculation of the isomerization efficiency in the film. A paradox in this procedure is that $\varepsilon_{\text{trans}}$ and ε_{cis} are necessary for the calculation of the degree of isomerization Y in eq 4, but if this degree of isomerization is unknown, then ε_{cis} cannot be calculated with eq 3. Fischer presented a procedure to overcome this problem and to determine the ratio $\varepsilon_{\text{cis}}/\varepsilon_{\text{trans}}$ by absorbance measurements at two different wavelengths⁵⁴ or through fluorescence measurements if only one of the two isomers shows a distinct fluorescence.⁵⁵

2.5. Positron Annihilation Lifetime Spectroscopy. The positron annihilation lifetime decay curves were measured at room temperature using an EG@G Ortec “fast–fast” lifetime spectrometer. A nickel-foil-supported [²²Na] sodium chloride radioactive positron source was used. Two stacks of film samples, each with a total thickness of about 1 mm, were placed on either side of the source. Measurements were performed in inert (nitrogen) atmosphere. The time resolution was 230 ps (full width at the half-maximum (fwhm) of the prompt coincidence curve). The contribution from annihilation in the source material, a background, and instrumental resolution were taken into account in the PATFIT program for treating the experimental lifetime data. The detailed procedures have been described elsewhere.^{56,57} The resulting data were determined as an average value from the several spectra collected for the same sample, having an integral number of counts of at least 10⁶ in each spectrum.

2.6. Inverse Gas Chromatography. The IGC methods is based on the measurement of the retention times and an estimation of the specific retention volumes V_g , as is described in more detail elsewhere.^{6,47} These values can be used for the determination of various thermodynamic parameters, including the activity coefficients at infinite dilution:

$$\ln\left(\frac{a_1}{w_1}\right)^{\infty} = \ln\left(\frac{RT}{V_g p_1^0 M_1}\right) - \frac{p_1^0}{RT}(B_{11} - V_1) \quad (5)$$

Here p_1^0 is the saturated vapor pressure of the solute; the second virial coefficient B_{11} (cm³/mol) and molar volume of the probe V_1 (cm³/mol) are used to allow for the nonideal character of

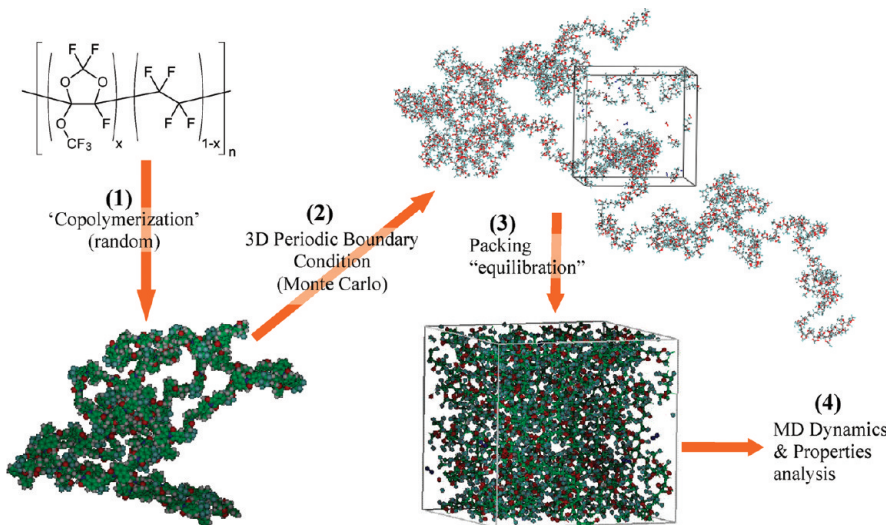


Figure 3. Construction procedure of atomistic packing models for Hyflon AD80X.

the probe. These parameters are calculated according to the recommendations presented in the handbook by Reid and Sherwood.⁵⁸ T is the test temperature, R is the universal gas constant, and M_1 is the molecular mass of the solute. The temperature dependence of the activity coefficients allows the estimation of the partial molar enthalpy of mixing $\overline{H}_1^{E,\infty}$:

$$\overline{H}_1^{E,\infty} = R \frac{\partial \ln \left(\frac{a_1}{w_1} \right)^{\infty}}{\partial (1/T)} \quad (6)$$

The object of the investigation was Hyflon AD80X because it was reported to have somewhat higher permeability^{59,60} than Hyflon AD60X, so diffusion limitations in the chromatographic experiment could be less detrimental. Hyflon AD80X was coated over the solid support Inerton AW from the solution in perfluorohexane: the stainless steel column with a length of 1.5 m and an inner diameter of 3 mm contained 0.19 g (about 3%) of the polymer. *n*-Alkanes C₆–C₁₂ were used as solutes. The low solubility of lower alkanes prevented the determination of their specific retention volumes and estimation of corresponding $\overline{H}_1^{E,\infty}$ values.

2.7. Molecular Dynamics Simulation Procedures. The molecular simulations were performed using the Materials Studio (4.0) software of Accelrys, Inc. (San Diego, CA). Amorphous polymer packings were constructed using the Theodorou/Suter method⁶¹ as implemented in the Amorphous-Cell module.⁶² The MD simulations were performed with the Discover software using the COMPASS force field.⁶³ The Materials Studio (4.0) software was run on a supercomputer (CINECA cluster, Bologna, Italy) and on PC hardware.

2.7.1. Generation and Equilibration of Polymer Structures. Both for Hyflon AD60X and for AD80X, three independent atomistic bulk models were prepared. The applied basic techniques of packing and equilibration have been described in detail elsewhere.^{52,64,65} The procedure is summarized in Figure 3. A brief outline of the procedure is given below, where the numbers refer to the different steps in Figure 3.

- (1) After preparing atomistic repeating units of TTD and TFE (see Scheme 1), a single copolymer chain with the appropriate molar ratio of TTD and TFE and with 770 repeat units (7856 atoms) for AD60X and 700 repeat units (8122 atoms) for AD80 was constructed, using conditional statistics. Since the experimental reactivity ratios for TTD and TFE were not available, a series of linear random chains were built by a trial and error procedure until the obtained composition (60 ± 1 mol % of TTD and 80 ± 2 mol % of TTD) was sufficiently

close to the specified experimental compositions of Hyflon AD60X and Hyflon AD80X, respectively. For the present work those chains with exactly 60.0 mol % of TTD (i.e., with 462 TTD units and 308 TFE units) for AD60X and with 80.0 mol % of TTD (i.e., with 560 TTD units and 140 TFE units) for AD80X were selected for the model construction.

- (2) For the initial packing of each Hyflon model, a polymer chain was grown under periodic boundary conditions at 308 K and at a density of about 15% of the experimental value in a simulation box. 600 Argon molecules were used as random obstacles to avoid ring catenations of the growing chain. Since solvent-cast films contain significant amounts of residual solvent⁶⁶ unless they are dried at temperatures above the T_g , a representative number of 41 solvent molecules were added in the Hyflon AD60X packing model and 26 molecules in Hyflon AD80X. In this way the model should correspond better to the experimental films, which were dried at only 50 °C to avoid degradation or thermal isomerization of the probe molecules. Three independent initial configurations were generated for each polymer. The chain was grown following the Theodorou/Suter method,⁶¹ based on the Rotational Isomeric State (RIS) model of the Amorphous Cell Program of Material Studio.⁶⁷ One single long chain was utilized to reduce the influence of chain ends on the simulations. This procedure to represent bulk amorphous systems is common and has been proven to be quite accurate in replicating the behavior of experimental polymeric systems.^{68,69}
- (3) The argon spacers were subsequently removed during the equilibration of the polymer models. The models were subjected to repeated sequences of energy minimization and dynamics runs at constant number of particles, temperature, and volume (NVT-MD), combined with force field parameter scaling. Subsequently, compression (runs at constant number of particles, temperature, and pressure, NpT-MD) and simulated annealing runs (NVT-MD dynamics at different temperature) of the initial packing were carried out through a set of successive MD simulations. This procedure yielded well-equilibrated packing models with stable density fluctuations at a density close enough to the given experimental value under the experimental pressure (1 bar). The following simulation conditions were used: periodic boundary condition to make the system numerically tractable and to avoid

Table 2. Properties of the Atomistic Packing Models for Three Samples of Each Hyflon Polymer

Hyflon model	no. solvent molecules	N_{atoms}^a	density, $\rho_{\text{simul}}(\text{g/mol})$	deviation ^b (%)	cell edge (Å)
AD60-1	41	8594	1.8933	-1.24	49.48
AD60-2	41	8594	1.8842	-1.71	49.55
AD60-3	41	8594	1.8900	-1.41	48.74
AD80-1	26	8122	1.8832	-1.81	49.57
AD80-2	26	8122	1.8925	-1.33	49.49
AD80-3	26	8122	1.8874	-1.59	49.53

^a Total number of atoms present in the box (polymer + solvent).
^b Experimental densities: 1.917 g/cm³ for AD60⁵² and 1.918 g/cm³ for AD80.²¹

symmetry effects; a cutoff distance of 22 Å for interaction energy functions with a switching function in the interval 20.5–22 Å. The Andersen thermostat⁷⁰ was used for temperature control, and the Berendsen method⁷¹ was applied to control the pressure of the system during NpT-MD simulations.

- (4) NpT-MD simulations were performed at $T = 298$ K and $p = 1$ bar for about 1 ns with the Discover package of Accelrys⁷² employing a time step of 1 fs for the numerical integration.

The obtained packing models have an edge length of about 50 Å, which offers a good compromise between calculation velocity and maximum void size that can be analyzed in comparison with boxes of 40 Å, often used in the literature. The aim of using larger cells in our study is to improve the statistics of the later-derived free volume data. Details are given in Table 2. The density of the simulated models deviate less than 2% from the experimental values for both Hyflon samples. These deviations are comparable to other simulated density data in the literature.⁶⁴

2.7.2. Free Volume Probing Method. Several definitions of free volume in glassy polymers are employed in the literature^{9,10} depending on the evaluation method or the subject under investigation.

For experimentalists the most common quantity is the FFV, derived from experimental densities. The FFV is the ratio of the “free volume” V_f of a polymer (cm³/g) and the specific volume V_{sp} , defined as reciprocal density:

$$\text{FFV} = V_f/V_{\text{sp}} \quad (7)$$

According to the Bondi method,⁷³ mostly used for such calculations, the free volume V_f can be estimated as

$$V_f = V_{\text{sp}} - 1.3V_{\text{vdW}} \quad (8)$$

where the van der Waals volume V_{vdW} is calculated using a group contribution method, and a universal “packing coefficient” equal to 1.3 is used to convert the van der Waals volume of the repeat unit in the “occupied” volume (cf. Supporting Information).

In this work, a “modified Bondi method” is also used, in which the *accessible free volume* is based on the insertion of a test particle. A recently developed computer program⁶⁹ was applied to estimate the size distributions of the FVEs. This gives more accurate information than the original semiempirical group contribution method to determine the occupied volume.⁷³ The calculation starts by the superimposition of a fine grid of about 0.5 Å over the cubic packing model. At every grid point, a hard sphere of a certain radius is inserted as a test particle. If the test particle overlaps with any atoms of the polymer matrix, which are also represented by respective hard spheres of van der Waals radii, the grid point is classified as “occupied”. If there is no overlap, the grid point is considered as “free” and the respective cublet contributes to the free volume. Neighboring free grid

points are collected into groups that represent individual holes. The grouping is done in two ways. In the first approach (named V_{connect}), affiliation to a group is defined through next neighborhood: every point of a group has at least one next neighbor that is also member of this group. This approach identifies holes, which may be of complex shape and of large volume. In a second approach (named R_{max}) for every “free” grid point, the “distance” to the nearest matrix atom is determined. Using a gradient procedure, all neighboring free grid points can be merged to a (local) set where all grid points are assigned to the same nearest local maximum in this “nearest distance” value. The R_{max} approach divides larger free volume regions of elongated or highly complex shape into smaller, more compact regions.

The second approach, originally introduced to match better the situation in PALS experiments where the positronium probe can obviously not completely sample very large holes of complex topology, also seems to be more adequate to depict the environment of a sorbed molecule. An oblong hole that is constricted at some point would be regarded as a single hole by the V_{connect} method. However, a penetrant molecule would have to jump an energy barrier to pass this bottleneck, and therefore it would “see” two separate sorption sites. By defining a hole according to the R_{max} method, this separation would be recognized.

The geometrical analysis of packing models allows the determination of a *fractional free volume*. The FFV accessible for a certain test particle in a packing model can be considered as the ratio of “free” grid points to the total number of grid points. This ratio depends very much on the selected radius value of the test particle. The highest value would be obtained for a test particle with vanishing radius. Recently, it was shown that this geometrical analysis of packing models gives FFV values in acceptable agreement with values found by the Bondi method if a hard sphere test particle is used with a radius of 0.473 Å.⁷⁴

3. Results and Discussion

3.1. Membrane Preparation. The most critical step in the membrane preparation procedure was the dissolution of the photochromic dyes in the perfluorinated matrix. While this step is usually straightforward in polymers such as polystyrene,¹⁶ poly(methyl methacrylate),²⁸ polycarbonate, and poly(vinyl acetate)²⁶ because of the possibility to use the same solvents for both the polymer and the dye molecule, no common solvents exist for the hydrocarbon photochromic dyes and the perfluorinated Hyflon AD polymers. This could compromise the possibility to prepare stable homogeneous polymer/dye solutions. In addition, the solid perfluoropolymer is normally also incompatible with the hydrocarbon photochromic dyes. Both problems were overcome successfully by the use of a solvent mixture and very low dye concentrations, so that highly transparent membranes were obtained, colorless or slightly colored, depending on the particular dye. For this purpose solubility tests of common organic solvents and HFE 7100 were carried out. It was found that dichloromethane was the best choice. It is a good solvent for the probe molecules; it is fully miscible with HFE at room temperature, and a 10 wt % Hyflon AD60X solution may contain at least 18 wt % of DCM without inducing phase separation of the polymer. In practice, much lower DCM concentrations are used during the membrane preparation procedure (< 1.5%). Finally, DCM is very volatile and will evaporate together with HFE 7100 from the nascent film.

Thus, mother solutions of the photochromic molecules in their most stable trans-isomer were prepared separately in DCM. The photochromic polymeric solutions were then prepared by addition of a small amount of this dye solution to the Hyflon AD solution under rapid stirring. Evaporation

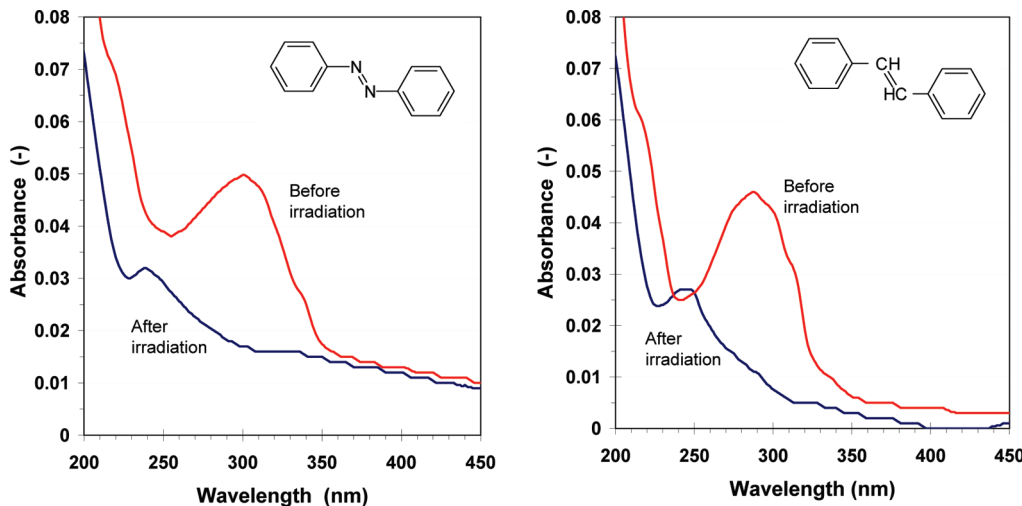


Figure 4. Absorption spectra of azobenzene and stilbene in Hyflon AD60X membranes, before and after photoirradiation at 350 nm for 15 min.

of the solution from a Petri dish or from a metal ring on a glass plate yielded completely transparent dense colorless or slightly colored photochromic films of about 60 μm thickness. Such films are sufficiently thick for spectroscopic analysis and for accurate time lag measurements of the most common gases except for the extremely fast helium and hydrogen. The total absence of any haze in the final films demonstrates that thanks to the low dye concentration in the polymer solution and to the increasing viscosity during evaporation of the solvent, the photochromic molecules could evidently be immobilized in the polymer matrix without noticeable aggregation. In all operations the exposure of the dyes to ambient light was minimized in order to prevent uncontrolled photoisomerization.

3.2. Photochromic Probe Method. *3.2.1. Reaction Kinetics and Progress of the Photoisomerization Reaction.* The common characteristic of the azobenzene and its derivatives is the clean and efficient photochemical isomerization that can occur about the azo bond when the chromophore absorbs a photon. The two states are a thermally stable trans and a metastable cis configuration. The cis configuration will then typically relax back to the trans state thermally with a lifetime that depends sensitively on the particular substitution pattern and on local conditions. Irradiation of the cis form with light within its absorption band can also induce the photochemical cis-to-trans isomerization (Figure 1). In the present work the extent of isomerization was determined spectrophotometrically, using a pure film without dye as a reference sample.

The extent of the photoisomerization, i.e., the maximum of the trans–cis conversion, depends strongly on the time of exposure at UV light. It is therefore very important to set the proper time of irradiation. For this purpose photochromic Hyflon AD membranes were irradiated at different times (5, 10, 15, and 20 min), and for each time of irradiation, a UV spectrum was recorded. Generally, the maximum absorbance was reached within 15 min of irradiation for all photochromic compounds. At room temperature the back-reaction in the films was sufficiently slow to allow normal manipulation and characterization of the film, provided that no uncontrolled light exposure occurs. Figure 4 shows two examples of the absorption spectra of the Hyflon AD60X membranes containing azobenzene and stilbene before and after irradiation.

3.2.2. Determination of Molar Absorption Coefficients. In all UV spectra of the photochromic films, the absorbance

was sufficiently low for the Lambert–Beer's law to be applicable. If the cis isomer did not have a maximum, its absorbance was read at the same wavelength of the peak maximum of the trans isomer; otherwise, the absorbance was read at its own peak maximum. The molar absorption coefficients of the cis and trans isomers in Hyflon AD membranes were thus calculated from eq 3, using the known dye concentration and optical path length, calculated from the measured membrane thickness and the original dye concentration in the casting solution. Details on the spectrophotometric analysis are given in the Supporting Information. The determination of the molar absorption coefficients of the probes in the Hyflon membranes was somewhat sensitive to noise compared to the analysis in solution due to the low probe concentration and the low membrane thickness. This is a common problem reported also for other membrane types.¹⁶

The progress of the azobenzene isomerization reaction generally depends strongly on its electronic environment and thus on the type of solvent³² or matrix used. In order to minimize the difference between the absorption measurements in film and in solution, all solution measurements were carried out in the perfluorinated solvent HFE. A certain amount of DCM was always needed for the preparation of the mother solution of the dye molecules and for guaranteeing their solubility also in the perfluorinated solvent.

3.2.3. Determination of the Total Isomerization Volume of the Photochromic Molecules and the FVE Size Distribution in the Films. A probe molecule has an associated van der Waals volume which represents volume occupied by the molecule, impenetrable for other molecules. This volume can be calculated using van der Waals radii tabulated by Bondi.⁷³ The extra volume needed by a dye molecule to isomerize is the volume swept by the van der Waals area, schematically displayed in Figure 2. *trans*-Azobenzene and stilbene are planar molecules, and their isomerization to the twisted cis isomer involves a complex series of motions which can only be elucidated by a combination of sophisticated analytical and computational techniques.⁷⁶ In the case of azobenzene and AZB derivatives the phenyl group is swept through a total angle of 114° during the inversion, and it twists 30° to assume the equilibrium conformation of the cis isomer.^{16,77} The volume required for isomerization consists of two components: the phenyl ring twist and the volume swept by the area comprised of the product of the phenyl thickness and the length. In the case of stilbene and stilbene derivatives, upon

Table 3. van der Waals Volume of Photochromic Probes and Extra Volume Needed To Isomerize

probe molecule	volume of the molecule, ^a Å ³	extra volume for isomerization, Å ³	total volume, ^b Å ³	ref
azobenzene	144	127	271	16
stilbene	151	222	373	16
Disperse Orange 3	171	250	421	this work
4,4'-dinitrostilbene	187	262	449	16
Disperse Red 1	207	310	517	this work
Disperse Orange 25	224	350	574	this work

^a According to Bondi's method.⁷³ ^b The sum of the van der Waals volume of the molecule and the extra volume.

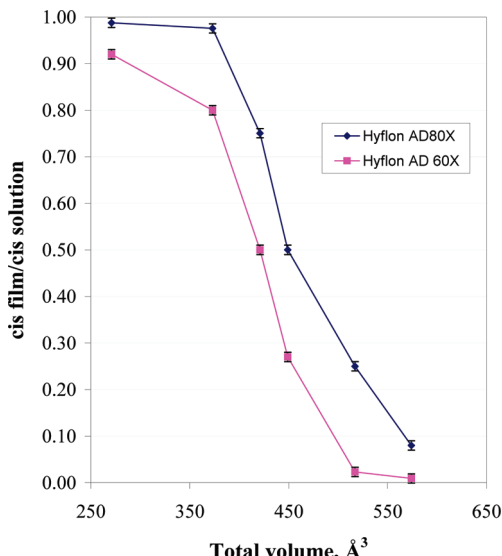


Figure 5. Ratio of the cis-isomer fraction in the film and the cis-isomer fraction in solution as a function of the total isomerization volume of the probes in Hyflon AD membranes.

irradiation, one of the central carbons twists 90° to the geometry of the excited state. The double bond disappears, allowing rotational diffusion about a single C–C bond.^{16,78,79} Viktor and Torkelson proposed a method to calculate the extra volume needed for isomerization, based on some simple geometrical considerations¹⁶ for a two-stage process: from the trans isomer to the excited state and from the excited state to the cis isomer. Table 3 lists the van der Waals volume of the photochromic molecules used in this work and the extra volume needed to isomerize, reported by Viktor and Torkelson or calculated according to their method.¹⁶

The size distribution of free volume elements can be derived from the degree of isomerization from the trans- to the cis-isomer (Y in eq 4). The ratio of the cis isomer fraction in the film and that in solution gives a quantitative measure of the efficiency of photoisomerization for each photochromic probe. Figure 5 shows this ratio as a function of the total isomerization volume of the dye molecules as defined in Table 3.

In both Hyflon grades the isomerization efficiency of the smallest probe, unsubstituted AZB, is nearly 100% and decreases rapidly with increasing probe size, down to about 0% for Disperse Orange 25. Thus, according to this method, the size of free volume elements ranges from about 250–520 Å³ in Hyflon AD60X and from ca. 380–600 Å³ in Hyflon AD80X. This means that, if we assume a spherical shape of the cavities, the averaged value of equivalent sphere radius ranges between 3.9 and 5.0 Å in Hyflon AD60X and

between 4.5 and 5.2 Å in Hyflon AD80X. These values are in line with the results reported on the basis of ¹²⁹Xe NMR studies.¹⁴ They confirm that Hyflon AD80X membranes possess only slightly bigger local FVEs than Hyflon AD60X. Arcella et al. reported a 3–6 times higher permeability of Hyflon AD80X than of AD60X.^{20,59} Recent data of some of the present authors on pure dense films suggest a much smaller difference between the two Hyflon grades,⁶⁰ in line with the small difference in the free volume found here.

3.2.4. Comments and Critical Remarks. The results of the photochromic probe method depend on various assumptions. For instance, a critical factor is the actual volume involved in the transition from the cis- to the trans-isomeric form of the probe molecules and vice versa. This volume is obtained by relatively simple approximations.¹⁶ A more accurate approach would ideally determine the true van der Waals volume and shape of the probe molecules by quantum chemical calculations in various stages of the isomerization reaction and in the transition state, requiring detailed knowledge of the excited state. This is beyond the scope of the present paper. Some limitations of the experimental analysis consist in the uncertainty of the isomerization efficiency in solution and in the precision of the determination of the molar absorption coefficient of the least stable isomer in solution when the thermal back-reaction is too fast to measure the photostationary state. For a number of different probe molecules the isomerization efficiency in solution varies roughly between 80% and 90%.¹⁶ An estimated average value of 85% was therefore used if no experimental data were available for a specific probe.

An important assumption in this method is that each probe molecule is isolated and that no clusters are formed in the polymer matrix. This requires a molecular solution of the probes in the polymer matrix. Although the probe molecules are in principle insoluble in the polymer matrix, the present paper describes an efficient method to circumvent this problem by the smart use of solvent mixtures. The extremely low probe concentration during solution casting and in the final polymer film, in combination with the low dipole moment of the trans-isomeric form of the probe molecules, makes clustering an unlikely event. The final probe concentration in the polymer film, ca. 1.7×10^{-6} mol/cm³, is less than 0.1 wt % and is negligible compared to the available free volume. Correspondingly, also the total number of probe molecules (ca. 10^{18} cm⁻³) is more than 2 orders of magnitude smaller than the FVE concentration, generally ranging from about 2×10^{20} to 7×10^{20} cm⁻³ for different polymers.¹⁰ We may therefore assume that the probes themselves do not contribute to the formation of free volume and that their distribution in the available free volume elements is completely at random.

3.3. Positron Annihilation Lifetime Spectroscopy. Since Hyflons exhibit a relatively high gas permeability, the measurements were carried out in a nitrogen atmosphere. This generally gives sufficiently accurate lifetimes compared to measurements carried out under vacuum, even for membrane materials and polymer sorbents with much longer lifetimes like PTMSP⁸⁰ and cross-linked polystyrenes.⁸¹ On the other hand, measurements in air showed significant quenching by oxygen in some samples and could therefore not be used. The PALS analysis was carried out on both grades, Hyflon AD60X and AD80X. It was found previously that the gas permeability of Hyflon AD60X membranes depends strongly on the sample preparation method, especially for larger penetrant molecules such as methane and CO₂.⁵² In particular, residual solvent in solution-cast films increases the gas permeability of these penetrants due to higher diffu-

Table 4. PALS Parameters of Hyflons in Terms of Three Components and the Equivalent Sphere Radii, R_3 , of Free Volume Elements (Measurements in N₂ Atmosphere)

copolymer	film preparation	τ_3 , ns	I_3 , %	R_3 , Å
AD80X	solution-cast ^a	5.80 ± 0.14	9.18 ± 0.38	5.22
	melt-pressed	4.58 ± 0.04	10.69 ± 0.18	4.63
AD60X	solution-cast ^b	5.02 ± 0.06	10.17 ± 0.21	4.78
	melt-pressed	4.36 ± 0.04	12.04 ± 0.21	4.51

^a From the solvent HFE 7100, dried 20 h at 50 °C. ^b From the solvent HFE 7100, dried for 20 h at 50 °C in vacuum.

sion coefficients. The latter is partially due to a certain degree of plasticization of the polymer by residual solvent, evidenced by the strong reduction of the T_g . The photochromic probe method requires a solution-casting procedure, and the limited thermal stability of some of the probe molecules in combination with the reluctance to release the residual solvent at low temperatures did not allow the preparation of samples which are completely free of residual solvent. Therefore, the PALS analysis in the present work was used to study the effect of residual solvent and the film formation procedure on the FVE size by comparing the data of solution-cast and melt-pressed films. Thus, in total four different samples were tested. It was shown that a good statistical fit with a maximum variance of about 1.01 can be obtained with the three-component PATFIT analyses of the lifetime distributions in all cases. The calculation procedures have been described elsewhere.⁸² If the statistics are sufficiently large, then similar methods (PATFIT, CONTIN, MELT, and LT) allow the evaluation of the entire void size distribution,^{46,83–85} but for the present analysis smaller statistics were available and only the average void size was determined by the finite term treatment. The main results are presented in Table 4.

Several interesting conclusions can be drawn by analyzing this table. First, for films prepared by the same procedure and under the same conditions, the lifetimes τ_3 of the copolymer Hyflon AD80X and the corresponding radii of FVE computed according to the Tao equation (eq 1) are always larger than those of Hyflon AD60X. This observation is in agreement with the higher cyclic dioxole comonomer content in Hyflon AD80X which reduces the packing efficiency of the polymer chains and, assumingly, increases the free volume. Also, previous studies that showed a higher permeability of Hyflon AD80X than that of Hyflon AD60X confirm this assumption.⁵⁹

Second, for both copolymers, the films obtained by solution-casting showed higher values of τ_3 and R_3 than the melt-pressed films. Thus, the radius of FVE for the solution cast film is more than 10% larger, while the difference in the corresponding spherical volumes amounts to more than 30%.

Some differences were observed in the intensities I_3 for both pairs of samples prepared via the solution-casting and the melt-pressing procedures. In fact, somewhat higher values of I_3 were observed for the melt-pressed samples. In a similar way, I_3 is larger for Hyflon AD60X samples than for Hyflon AD80X. In similar systems where spur processes may be nearly the same, it has been suggested⁸⁶ to use the I_3 values for estimation of the relative fractional free volume from the elementary free volume v_f as

$$\text{FFV} = Cv_f I_3 \quad (9)$$

where C is a proportionality factor which must be estimated from independent data. I_3 depends not only on the concentration of FVEs but also on the material type, the probability

of formation of o-Ps, the rate of capture of o-Ps by FVE, and the possible quenching by polar groups, e.g., in polyimides. In very similar materials, as for the two Hyflon grades and for the samples prepared from the same materials but under different conditions, the equation can be used for a qualitative estimation of their relative fractional free volumes. In the samples studied, the differences in I_3 are not big enough to make a final quantitative conclusion for the value of FFV, but nevertheless, these results suggest that the larger FVE size in Hyflon AD80X compared to Hyflon AD60X (for the same membrane preparation procedure) and in the solution-cast samples compared to the melt-pressed samples (for the same Hyflon grade) are compensated by a lower FVE concentration. Indeed, the densities of both grades of Hyflon are reported to be similar,^{21,52} which suggests a more or less equal FFV. Also, Bondi's method yields a nearly identical FFV for both samples.

The transport properties depend not only on the FVE size distribution but also on the interconnectivity of the free volume elements and on the chain dynamics. Information on the interconnectivity is obtained from MD simulation studies (see below). The chain dynamics are correlated with, for instance, the T_g of the polymer, which in turn depends on the dioxole comonomer content and on the presence of residual solvent.

For a solution-cast film of the more permeable polymer, Hyflon AD80X, a test for possible oxygen-induced quenching was carried out by comparison of measurements in air and in N₂ atmosphere. Indeed, the presence of O₂ induced a noticeable decrease in the observed τ_3 values: the positronium lifetime in the presence of air was 5.24 ns, about 0.6 ns shorter than in nitrogen atmosphere. Meanwhile, the observed intensity $I_3 = 9.39 \pm 0.11$ was virtually the same in air and in nitrogen atmosphere. Although chemical quenching or conversion of Ps by O₂ generally affects not only τ_3 but also I_3 , the latter was not observed in the present case, confirming that the results can only be used for a qualitative comparison. As discussed above, a constant value of I_3 would normally suggest that the FVE concentration does not change notably. In any case, only the measurements in a N₂ atmosphere were used for the FV analysis.

3.4. Inverse Gas Chromatography. Studies of different glassy polymers indicated that for solutes (*n*-alkanes C₃–C₁₂) having different molecular size the $\overline{H}_1^{E,\infty}$ values initially decrease as the molecular size (e.g., its critical volume V_c) increases, passing through a minimum at a particular size of the solute molecules (these sizes are different for different polymers), and then increase again.⁹ It is important that strongly negative values of the enthalpy of mixing $\overline{H}_1^{E,\infty}$ are observed. This implies that the process of mixing in glassy polymers (in contrast to rubbers) does not require overcoming the work of chain displacement. Exothermic mixing is consistent with the idea that the solute molecules of certain size can be accommodated within the FVE. This hypothesis is substantiated by establishment of correlations between the minimum $\overline{H}_1^{E,\infty}$ values and the diffusion coefficients and gas permeability of glassy polymers.⁹ Thus, the IGC method allows estimation of the FVE size in glassy polymers.

The dependence of $\overline{H}_1^{E,\infty}$ in Hyflon AD80 on the size of the solutes (*n*-alkanes) is shown in Figure 6. For comparison, the data for two other glassy polymers (polyvinyltrimethylsilane, PVTMS,¹³ and amorphous Teflon AF1600)⁸⁷ and same set of solutes are also shown. It can be noted that the mixing of these molecular probes is strongly exothermic in Hyflon AD80. When the size of the solutes decreases from dodecane to hexane, the values of $\overline{H}_1^{E,\infty}$ decrease. Unfortu-

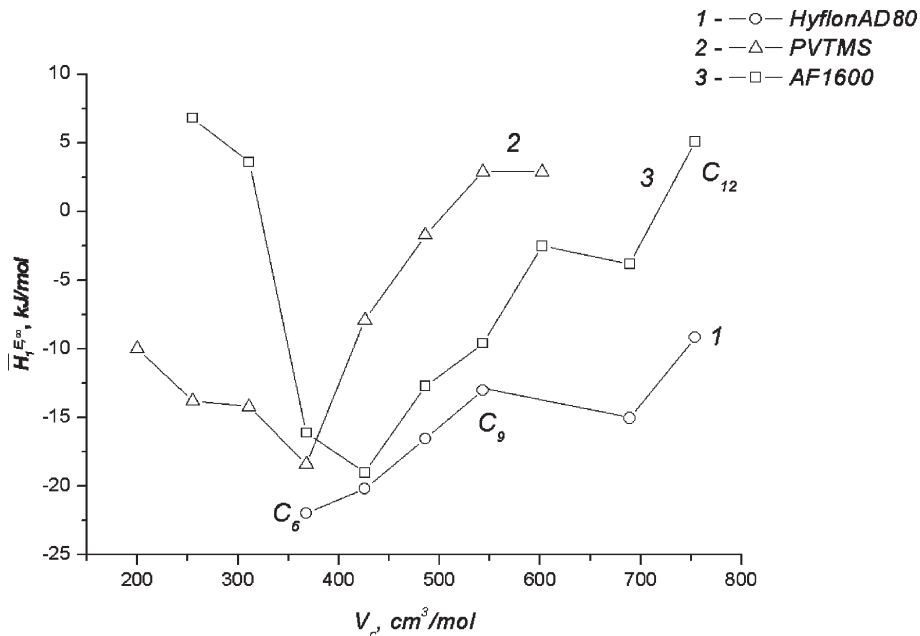


Figure 6. Dependence of $\bar{H}_1^{E,\infty}$ on the critical volume of *n*-alkane solutes in Hyflon AD80X.

nately, the solubility of the alkanes lower than C_6 was so small that it was impossible to locate the minimum of the curve $\bar{H}_1^{E,\infty}$ vs V_c . It can only be stated that the minimum value of $\bar{H}_1^{E,\infty}$ in this polymer is equal to or smaller than $368 \text{ cm}^3/\text{mol}$ (critical volume of *n*-hexane according to ref 58). Such value is consistent with relatively low gas permeability of Hyflon AD: the largest coordinate of minimum $\bar{H}_1^{E,\infty}$ is observed for Teflon AF1600 which has a permeability coefficient $P(\text{O}_2) = 170$ barrer,¹⁷ for PVTMS the following values are characteristic: $V_{c(\min)} = 368 \text{ cm}^3/\text{mol}$, $P(\text{O}_2) = 44$ barrer. The reported $P(\text{O}_2)$ value for a solution-cast Hyflon AD80X sample is 42 barrer,⁶⁰ so it can be assumed that its $V_{c(\min)}$ should indeed be similar to that of PVTMS.

It should be taken into account that the plot shown in Figure 6 is a correlation. Different scales can be chosen for the size of the molecular probes. It has been shown that similar correlations can be obtained for the critical volume V_c and for the molecular volume V_b in the liquid phase at corresponding boiling point as the scaling parameters.⁸⁸ Hence, if one supposes that the smallest observed value of $\bar{H}_1^{E,\infty}$ is the upper limit for the size of FVE in Hyflon AD80, it gives the following upper limits for the radii of spherical FVEs:

3.5. Molecular Dynamics Simulations. 3.5.1. Generation and Equilibration of Polymer Structures and Qualitative Free Volume Evaluation. The simulated atomistic bulk models of both Hyflon AD80X and Hyflon AD60X with a representative number of residual solvent molecules allow an accurate determination of the characteristics of the structure of chain packing, the related free volume, and their distributions. A qualitative visualization of the free volume distributions for the packing models is shown in Figure 7. The simulation cells of both Hyflon samples have been cut into slices of about 5 \AA thickness perpendicular to the respective z -axis. Eight of the 10 slices of the boxes are displayed in Figure 7, which gives a qualitative visual impression of the difference between the two copolymers. Hyflon AD80X slices contain larger areas of free volume compared to AD60X. This is in good agreement with the lower gas permeability in AD60X.⁶⁰ In comparison, the voids are significantly smaller

than those found by Hofmann et al. in Teflon AF2400 and AF1600, with lateral void widths between ca. 5 and 20 \AA .⁴⁹ This corresponds again to the lower gas permeabilities in the Hyflons compared to Teflons AF.

The shape of the free volume elements in each slide is irregular and usually nonspherical. They are rather large, and the elongated FVE elements may extend across several slices. This characteristic is more evident in AD80X than in AD60X.

As for other high free volume and high permeability polymers (i.e., PTMSP and aged PTMSP, Teflon AF2400, AF1600),⁴⁹ the two Hyflon polymers are characterized by the presence of two qualitatively different states. They contain regions of high segmental packing density where the free volume distribution resembles that of conventional glassy polymers⁸⁹ and regions with rather large voids. In the case of perfluoropolymers these free volume areas show a much smaller tendency to form a continuous hole phase than in PTMSP.⁴⁹

The results of the free volume analysis by the V_{connect} and R_{\max} methods are visualized qualitatively in Figure 8 for a representative slice of Hyflon AD80X. The polymer matrix atoms are displayed in "stick style". Every free grid point is presented by a sphere of radius of 1.1 \AA representing the positronium-sized test particle. It should be noted that some matrix atoms as well as FVEs appear fragmented due to the slicing process or continue on the opposite side due to the periodic boundary conditions (double-headed arrow).

The left side of Figure 8 shows the result for the V_{connect} analysis. The overlapping spheres build the FVEs. Except for the very small elements in light green, all spheres of one color belong to the same FVE. The largest FVE in this model is indicated in dark red. It seems to consist of eight separate parts, but these parts belong to one single very large interconnected free volume region which extends over the neighboring slices and which would be accessible for the test particle. This single FVE represents about 80% of the accessible free volume. It is a kind of randomly connected channel and cavity system, definitely not a big spherical pore. All larger cavities or channel sections can be split into smaller more spherical segments with the R_{\max} method, as shown in

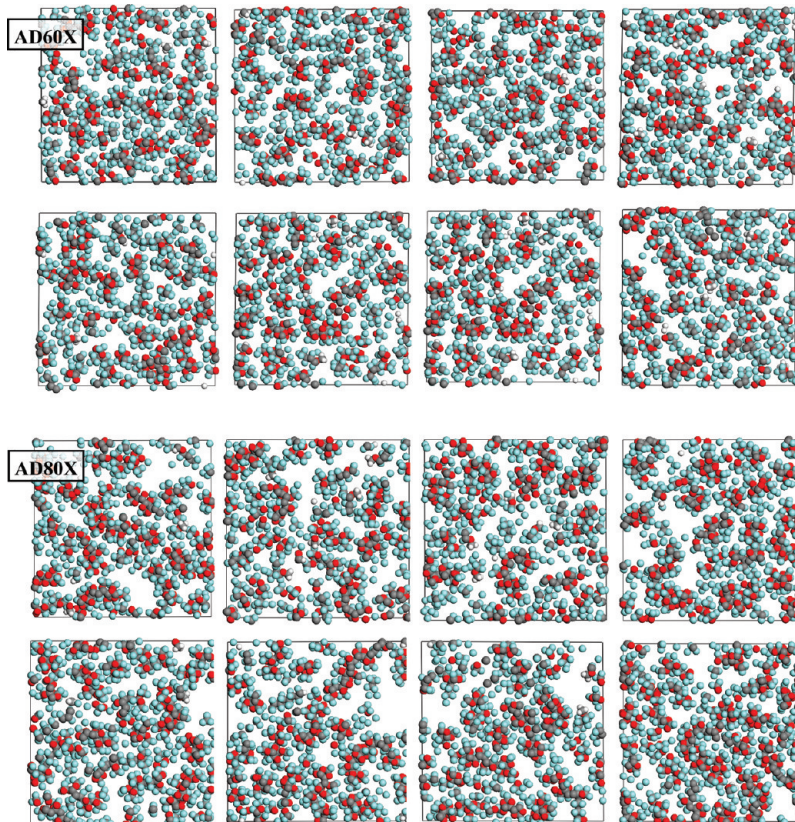


Figure 7. A $50 \times 50 \text{ \AA}^2$ sliced box model of Hyflon AD60X (top) and Hyflon AD80X (bottom). Slice order from left to right and from top to bottom.

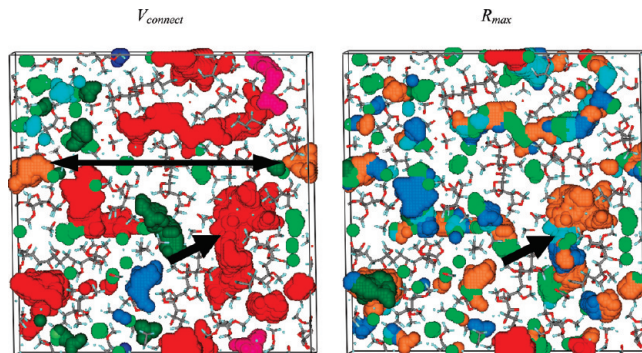


Figure 8. Representative slice of about 5 \AA thickness of one atomistic packing of Hyflon AD80X, showing the free volume elements according to the V_{connect} and the R_{max} method for the positronium probe ($r = 1.1 \text{ \AA}$). In the V_{connect} method (left) each color indicates one single FVE, associated with free grid points. In the R_{max} method (right) every single free volume element is subdivided into smaller ones, indicated with different colors. The polymer matrix is represented by the colored sticks.

the right graph of Figure 8. A good example is again the very large cavity indicated with the single arrow. The R_{max} method splits it into about five smaller segments of more compact and nearly spherical shape.

3.5.2. Quantitative Analysis of the Free Volume Distribution. The size distributions of FVEs from the packing models have been calculated with the V_{connect} and R_{max} approach for every packing model (see Table 5). Figure 9 shows the distributions for both Hyflon AD60X and Hyflon AD80X as an average of three packing models in comparison with the results of the experimental methods. The analysis was performed using a grid spacing of 0.5 \AA and a positronium sized test particle with a radius of 1.1 \AA . The volume of each FVE

Table 5. Maximum Estimated FVE Equivalent Sphere Radius in a Solution-Cast Hyflon AD80X Sample Determined by IGC

V_c				V_b		
	cm^3/mol	$\text{\AA}^3/\text{molecule}$	$R_{\text{eq},c}, \text{\AA}$	cm^3/mol	$\text{\AA}^3/\text{molecule}$	$R_{\text{eq},b}, \text{\AA}$
368	611	5.3	235	392	4.5	

is represented by the radius of a volume-equivalent sphere, R_{eq} , calculated as

$$R_{\text{eq}} = \sqrt[3]{\frac{3}{4\pi} V} \quad (10)$$

where V is the void volume.

The analysis with the V_{connect} method confirms the qualitative impression of the slices in Figure 7. For a positronium sized test particle, every packing model contains one large interconnected region, indicated by one of the three single columns in the size range between 14 \AA and 21 \AA (equivalent sphere radius), plus several more individual large pores of $\geq 7 \text{ \AA}$. An additional set of smaller independent holes with a radius between 1.1 \AA and about 7 \AA represents numerically the largest fraction, although their total volume is small. Here, it should be emphasized that a radius of for instance 15 \AA does not imply that the packing model contains a single huge spherical hole of this size because the “radius” of the volume equivalent sphere is only a measure for the total extension of this interconnected “cave and channel system”. From the comparison of the V_{connect} distribution of both Hyflons, it follows that the interconnected FVEs in AD80X are a bit larger than in AD60X. A similar bimodal distribution was also found in analogous simulations of Teflons AF⁴⁹ and with the newly developed alternative CESA algorithm of Willmore et al.⁹⁰

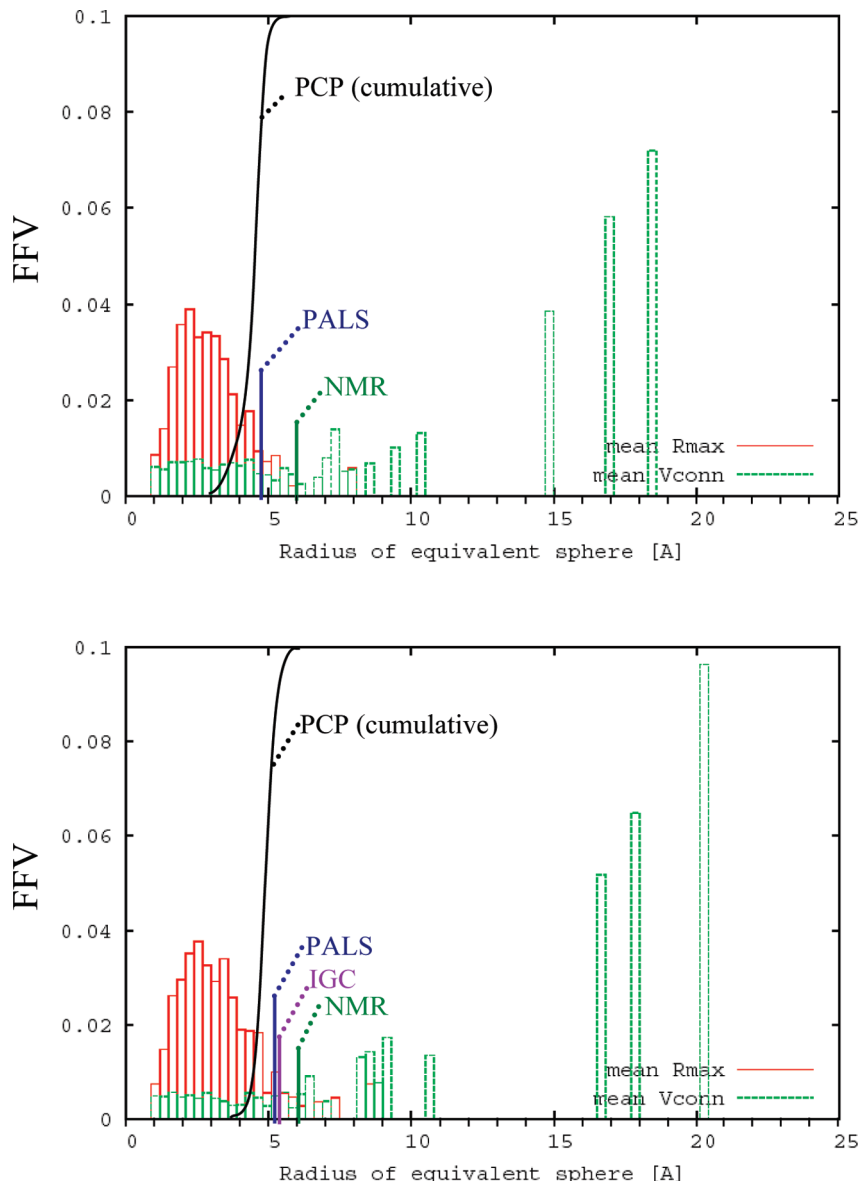


Figure 9. Overview of the FVE equivalent sphere radius distribution in Hyflon AD60X (top) and Hyflon AD80X (bottom). Bar chart: FVE distributions by MD simulations with a probe radius of 1.1 Å (R_{max} and V_{connect} methods, average of three packing models). The average values determined by PALS, the maximum value for IGC based on the probe critical volume, and the reference value from ¹²⁹Xe NMR spectroscopy for a spherical void¹⁴ are also indicated as a vertical line. The sigmoidal curve represents the cumulative distribution by the PCP method, obtained from the smoothed data of Figure 5.

Since the R_{max} approach splits neighboring FVEs into smaller more compact and more spherical parts, one obtains distributions with radius values between 1.1 and 5 Å with a distribution maximum between 2.0 and 3.0 Å for both Hyflons.

Recently, some authors argued that the effective size of the o-Ps probe (typically assumed to have a radius of 1.1 Å) is too small to simulate correctly the localization of the o-Ps, and they suggested that the effective size should be increased to a radius of about 1.5 Å¹⁹ and references included. Therefore, the V_{connect} and R_{max} analysis was also carried out with a probe radius of 1.5 Å. On the basis of the obtained distributions the mean FVE radius was calculated for a quantitative comparison with the experimental results. The total accessible volume and the FFV calculated with both probe sizes are listed in Table 6. The FFV obtained by Bondi's method (section 3.5.3) is indicated for comparison.

The mean FVE radius, R_{eq} , is determined from the total accessible volume and the mean number of detected holes in the respective packing models.

$$R_{\text{eq}} = \sqrt[3]{\frac{3}{4\pi} \frac{V_{\text{acc}}}{n}} \quad (11)$$

where n is the total number of holes. The results are given in Table 7.

With a probe of 1.1 Å the V_{connect} approach finds in the three packings of AD60X an average of 395 ± 41 holes, forming an accessible free volume of about $40\,600 \text{ \AA}^3$ and corresponding to a mean radius of $2.91 \pm 0.10 \text{ \AA}$. In AD80X the accessible free volume is 11% higher, but the number of holes is 20% lower than in AD60X, resulting in a larger mean radius of about 3.25 \AA . The geometrical splitting of larger free volume regions into smaller parts (R_{max} approach)

Table 6. Simulated Amount of Accessible Volume and of Fractional Free Volume for AD60X and for AD80X, Calculated for a Probe Equivalent Sphere Radius of 1.1 and 1.5 Å, and Estimated with Bondi's Methods

Hyflon	FV	probe $r_p = 1.1 \text{ \AA}$		probe $r_p = 1.5 \text{ \AA}$		Bondi's method	
		value	std dev	value	std dev	traditional	modified
AD60X ^a	$V_{\text{acc}} [\text{\AA}^3]$	40600	1460	24150	2370		
AD60X	FFV	0.338	0.012	0.202	0.023	0.23	0.226
AD80X ^a	$V_{\text{acc}} [\text{\AA}^3]$	45300	650	33940	2170		
AD80X	FFV	0.373	0.005	0.279	0.017	0.23	0.239

^a Box size $119530 \pm 3250 \text{ \AA}^3$ for Hyflon AD60X and $121510 \pm 294 \text{ \AA}^3$ for Hyflon AD80X (average of three packing models).

Table 7. Estimated Description of FVEs from the Simulated Packing Models (Average Values for Three Boxes)

Hyflon	FV approach	probing $r_p = 1.1 \text{ \AA}$		probing $r_p = 1.5 \text{ \AA}$		void probing $r_p = 1.1 \text{ \AA}$, evaluation $r_{\text{eq}} = 1.5 \text{ \AA}$		
		total no. of holes	mean $R_{\text{eq}} [\text{\AA}]$	total no. of holes	mean $R_{\text{eq}} [\text{\AA}]$	no. holes ^a with $R_{\text{eq}} \leq 1.5 \text{ \AA}$	eff no. of holes with $R_{\text{eq}} > 1.5 \text{ \AA}$	corrected mean $R_{\text{eq}} [\text{\AA}]$
AD60X	V_{connect}	395 ± 41	2.91 ± 0.10	224 ± 12	2.95 ± 0.13	226 ± 18	169 ± 24	3.87 ± 0.19
AD60X	R_{max}	1087 ± 88	2.08 ± 0.05	421 ± 23	2.39 ± 0.10	432 ± 31	655 ± 57	2.46 ± 0.06
AD80X	V_{connect}	317 ± 26	3.25 ± 0.10	172 ± 18	3.62 ± 0.20	199 ± 22	119 ± 9	4.50 ± 0.13
AD80X	R_{max}	1009 ± 76	2.21 ± 0.06	439 ± 21	2.64 ± 0.10	385 ± 38	624 ± 47	2.59 ± 0.07

^a Corresponding to < 8% of the total accessible volume when measured with a 1.1 Å equivalent sphere radius probe.

Table 8. Overview of the Average Free Volume Element Sizes According to Different Experimental Probing Techniques in Hyflon AD Membranes

sample	method	average FVE equivalent sphere radius, R (Å)					
		PALS	PCP	IGC	^{129}Xe NMR ¹⁴		
		R_3	R_{eq}	$R_{\text{eq},c}^b$	$R_{\text{eq},b}^c$	R_{eq}	$R_{\text{eq,cyl}}^d$
AD60X solution-cast		4.78	4.64			6.0	4.1
melt-pressed		4.51 ^a					
AD80X solution-cast		5.22 ^a	4.79	≤ 5.3	≤ 4.5	6.12	4.16
melt-pressed		4.63 ^a					

^a Measurement in N_2 . ^b Based on probe critical volume. ^c Based on probe molecular volume in the liquid at the boiling point. ^d Value for cylindrical instead of spherical pore shape.

increases the number of pores considerably and results in lower mean pore radii of about 2.08 and 2.21 Å for AD60X and AD80X, respectively. These values are considerably lower than the experimental values (Figure 9 and Table 8), while the FFV is significantly overestimated compared to the value of 23% obtained by Bondi's method.

The analysis with a larger probe of 1.5 Å gives some improvement, with an increase of the average FVE size and a strong reduction of V_{acc} and FFV to a somewhat lower value (AD60X) or a slightly higher value (AD80X) than predicted by Bondi. It is interesting to note that with the V_{connect} method and the 1.5 Å probe the number of pores in AD80X is lower than in AD60X, while its accessible volume is higher. This reflects a larger number of isolated voids in the latter and the stronger interconnection of the FVEs in AD80X. Nevertheless, the increase of the average FVE equivalent sphere size is still relatively small when a probe with a radius of 1.5 Å is used. Even the values calculated according to the V_{connect} method, which usually gives the highest results, are still considerably lower ($R_{\text{eq,AD60X}} = 2.95 \text{ \AA}$ and $R_{\text{eq,AD80X}} = 3.62 \text{ \AA}$, respectively) than the experimental values.

A better correspondence with simulated and experimental results is obtained if the overall free volume is determined with a o-Ps-size probe with a radius of 1.1 Å, whereas the smallest detected voids with an equivalent sphere radius of less than 1.5 Å are excluded for the calculation of the average size (right columns in Table 7). The motivation is that o-Ps particles have a too high probability to be annihilated by the

wall in so small voids, especially if the latter are relatively thin and elongated. Although the number of excluded pores with $R_{\text{eq}} \leq 1.5 \text{ \AA}$ is relatively large, they do not account for more than about 6–8% of the total V_{connect} void volume because of their small individual volume. Therefore, with this procedure the average equivalent sphere diameter of FVEs according to the V_{connect} method increases to 3.87 and 4.53 Å for AD60X and AD80X, respectively. These values are much closer to the experimental data. However, the physical basis of such reasoning is somewhat weak, and further improvement of the method is necessary. In any case, all calculations of Table 7 show larger mean radii for the FVEs in AD80X than in AD60X.

3.5.3. Modified Bondi Method. The modified Bondi method also allowed a quantitative analysis of the FFV of the samples. As described in section 2.7.2, the FFV according to the modified Bondi method was calculated from the above packing models, using a test particle of a radius of $r = 0.473 \text{ \AA}$. The thus-obtained FFV was 0.239 ± 0.003 for AD80X, compared to 0.226 ± 0.004 for AD60X, confirming the slightly higher FFV for Hyflon AD80X.

It must be noted that the FFVs obtained by the computational methods cannot be compared on an absolute scale. In the modified Bondi method, the radius of the test particle ($r = 0.473 \text{ \AA}$) is smaller than the grid size (0.5 \AA), whereas for the calculation with a positronium-like test particle, the radius is much larger than the grid size. In that case a single free grid point may represent a free volume segment that has at least the volume of the test particle. If the same hole is analyzed with the Bondi test particle, it may be represented by about 27 free grid points. The calculation procedure tries to account for these effects in approximation. The deviation is larger if a packing model contains many small holes. The FFV determined by the traditional (Supporting Information) and modified Bondi method are in good mutual agreement (Table 6) but considerably higher than the void volume fraction of 9.4–9.5% reported previously.²⁰

4. Comparison of the Methods and Conclusions

The present paper describes the investigation of the free volume in amorphous glassy perfluoropolymer films of Hyflon AD. To the knowledge of the authors this is the most extensive comparative study of all actively used experimental methods, namely PALS, IGC, and ^{129}Xe NMR spectroscopy, for probing

of the free volume in a single type of a glassy polymer. The study further includes the photochromic probe method, and it is demonstrated that this method can be successfully used to determine the FVE size distribution in amorphous glassy perfluoropolymers. In addition, the experimental findings are considered jointly with the results of computational studies of the polymer packing and of the free volume and free volume size distribution and spatial arrangement in the investigated Hyflon polymers.

Each of the investigated methods “senses” the free volume in another specific way, with probes of different size and properties, and each method provides a different level of detail in the obtained results. By and large, the agreement between the various experimental methods and between the experimental versus computational results is reasonable.

The strengths and weaknesses of the different experimental techniques and computational methods were indicated. PALS allows the best experimental probing of the FV distribution due to the small size of the *o*-positronium particles, but in contrast to the MD simulations it can only probe the volume and to some extent the shape but not the connectivity of the FVEs. The PCP method has the advantage of its simplicity, but it has also the strongest limitations: the probes have a distinct, nonspherical shape, related to the structure of the dye molecule, and the minimum size which can be probed is that corresponding to azobenzene, the smallest available probe molecule. In spite of the differences and limitations of each technique, there is a surprisingly good agreement of the results from all methods if the FVE size is expressed as the radius of an equivalent sphere.

In quantitative terms the results of the photochromic probe method were in rather good agreement with those of the other experimental FV probing techniques PALS and IGC, and with ^{129}Xe NMR reported in the literature,¹⁴ although in the approximation of spherical microcavities PALS gives somewhat higher R values than PCP. On the other hand, the results of IGC may be in better agreement with the PCP data if the FVE size is based on the probe volume at the boiling point, while they are closer to the PALS data if the probe critical volume is considered. With respect to the other techniques, the photochromic probe method revealed a particularly narrow FVE size distribution. This is probably a limit of the PCP method, which requires free volume elements not only of a certain size but also of a certain shape, in order to have sufficient freedom of motion for the probe molecules to undergo isomerization. Such information on the shape and interconnectivity of the FVEs was only obtained by MD simulations. These indeed confirmed that many voids have a narrow and extended shape. The MD method revealed a rather wide FVE size distribution. Depending on the calculation method, the MD simulations seem to underestimate the average FVE size found by the other techniques, especially in terms of R_{\max} . This is related to the fact that experimental techniques are much more sensitive to the void shape than MD, for which an equivalent sphere size can be defined without any physical implications. In real PALS measurements the quenching probability of the probe strongly depends on the void geometry, and it is higher in a thin elongated pore than in a spherical pore of the same volume. Very narrow pores may not be detected at all or may be detected as very small, while such pores may be small or large according to MD, depending on their degree of interconnectivity. The importance of the pore shape is confirmed by the better correspondence of the NMR results with the other experimental methods when a cylindrical pore shape is considered than when a spherical shape is considered. Normally the experimental methods should detect an intermediate average void size compared to the two MD evaluation methods (V_{connect} and R_{\max}). If this is not the case, this may be due to the approximations used in the MD simulations, for instance in the force field used. In any case, the present study

indicates that the pore shape is a fundamental parameter and that a description of the FVE size distribution in terms of the pore size alone is too restrictive. In the PALS experiments, for the same lifetime τ_3 , processing of the results in terms of channel or slit geometries makes the width of the pore smaller (about 1.2 times for the channel and 1.7 times for the slit) and thus the coincidence with the most probable pore width found by MD simulation (R_{\max} approximation) better.³⁹

An overview of the main results from the different techniques is given in Table 8. The mean FVE sizes from all experimental techniques are in between the peak maxima from the R_{\max} and V_{connect} MD simulation approaches (Figure 9). Summarizing, it may be concluded that all methods detect a slightly higher average FVE size in Hyflon AD80X compared to Hyflon AD60X, and this is in agreement with the ^{129}Xe NMR data reported in the literature.¹⁴ On the other hand, there seems to be no substantial difference in the FFV of the two polymer grades according to MD. This is again confirmed by ^{129}Xe NMR spectroscopy, which indicates an equal xenon solubility in both polymers, $0.19 \text{ cm}^3 \text{ STP}/(\text{cm}^3 \text{ atm})$.¹⁴

One of the main conclusions of this work is that for a fair comparison of the different approaches a discussion on the shape of the FVEs is of fundamental importance. MD is the only method which can provide such information directly. Knowledge of the FVE size and shape distribution is helpful for the understanding of numerous molecular properties of polymeric materials, for instance for the understanding of mass transport in these polymers when used as a membrane material.

Acknowledgment. Parts of the work were financed by the European Commission 6th Framework Program Project Multi-MatDesign “Computer aided molecular design of multifunctional materials with controlled permeability properties” (Contract NMP3-CT-2005-013644) and the Italian Ministry of Education, University and Research, Project FIRB-CAMERE (Contract RBNE03JCR5). Solvay-Solexis is gratefully acknowledged for providing the free sample of Hyflon AD80X. We thank Giorgio De Luca for the drawings of the molecular structures of the photochromic probes and for the calculations of the probe isomerization volume.

Supporting Information Available: Spectroscopic data and determination of the free volume by Bondi's group contribution method. This material is available free of charge via the Internet at <http://pubs.acs.org>.

References and Notes

- Huang, Y.; Paul, D. R. Physical aging of thin glassy polymer films monitored by gas permeability. *Polymer* **2004**, *45*, 8377–8393.
- Robertson, R. E. Segmental Mobility in the Equilibrium Liquid below the Glass Transition. *Macromolecules* **1985**, *18*, 953–958.
- Chow, T. S. Kinetics of Free Volume and Physical Aging in Polymer Glasses. *Macromolecules* **1984**, *17*, 2336–2340.
- Curro, J. G.; Lagasse, R. R.; Simha, R. Diffusion Model for Volume Recovery in Glasses. *Macromolecules* **1982**, *15*, 1621–1626.
- Thran, A.; Kroll, G.; Faupel, F. Correlation between fractional free volume and diffusivity of gas molecules in glassy polymers. *J. Polym. Sci., Part B: Polym. Phys.* **1999**, *37*, 3344–3358.
- Nagel, C.; Günther-Schade, K.; Fritsch, D.; Strunskus, T.; Faupel, F. Free volume and transport properties in highly selective polymer membranes. *Macromolecules* **2002**, *35*, 2071–2077.
- Nagai, K.; Masuda, T.; Nakagawa, T.; Freeman, B. D.; Pinna, I. Poly[1-(trimethylsilyl)-1-propyne] and related polymers: synthesis, properties and functions. *Prog. Polym. Sci.* **2001**, *26*, 721–798.
- Polyakov, A. M.; Starannikova, L. E.; Yampolskii, Yu. P. Amorphous Tefflons AF as organophilic pervaporation materials: Transport of individual components. *J. Membr. Sci.* **2003**, *216*, 241–256.
- Yampolskii, Yu. P. Methods for investigation of the free volume in polymers. *Russ. Chem. Rev.* **2007**, *76*, 59–78.

- (10) Yampolskii, Y.; Shantarovich, V. Positron annihilation lifetime spectroscopy and other methods for free volume evaluation in polymers. In *Materials Science of Membranes for Gas and Vapor Separation*; Yampolskii, Yu., Pinna, I., Freeman, B. D., Eds.; John Wiley & Sons: Chichester, England, 2006; Chapter 6, pp 191–210.
- (11) Shrader, D. M.; Jean, Y. C. *Positron and Positronium Chemistry*; Elsevier: Amsterdam, 1988.
- (12) Dlubek, G.; Clarke, A. P.; Fretwell, H. M.; Dugdale, S. B.; Alam, M. A. Positron lifetime studies of free volume hole size distribution in glassy polycarbonate and polystyrene. *Phys. Status Solidi A* **1996**, *157*, 351–364.
- (13) Yampolskii, Y. P.; Kaliuzhnyi, N. E.; Durygarian, S. G. Thermodynamics of sorption in glassy poly(vinyltrimethylsilane). *Macromolecules* **1986**, *19*, 846–850.
- (14) Golemmé, G.; Nagy, J. B.; Fonseca, A.; Algieri, C.; Yampolskii, Y. ¹²⁹Xe-NMR study of free volume in amorphous perfluorinated polymers: comparison with other methods. *Polymer* **2003**, *44*, 5039–5045.
- (15) Yampolskii, Y. P.; Shantarovich, V. P.; Chernyakovskii, F. P.; Kornilov, A. I.; Platé, N. A. Estimation of free volume in poly(trimethylsilyl propyne) by positron annihilation and electrochromism methods. *J. Appl. Polym. Sci.* **1993**, *47*, 85–92.
- (16) Victor, J. G.; Torkelson, J. M. On measuring the distribution of local free volume in glassy polymers by photochromic and fluorescence techniques. *Macromolecules* **1987**, *20*, 2241–2250.
- (17) Alentiev, A. Yu.; Yampolskii, Yu. P.; Shantarovich, V. P.; Nemser, S. M.; Platé, N. A. High transport parameters and free volume of perfluorodioxole copolymers. *J. Membr. Sci.* **1997**, *126*, 123–132.
- (18) Merkel, T. C.; Pinna, I.; Prabhakar, R.; Freeman, B. D. Gas and vapor transport properties of perfluoropolymers. In *Materials Science of Membranes for Gas and Vapor Separation*; Yampolskii, Yu., Pinna, I., Freeman, B. D., Eds.; John Wiley & Sons: Chichester, England, 2006; Chapter 9.
- (19) Rudel, M.; Kruse, J.; Rätzke, K.; Faupel, F.; Yampolskii, Yu. P.; Shantarovich, V. P.; Dlubek, G. Temperature dependence of positron annihilation lifetimes in high permeability polymers. Amorphous Teflons AF. *Macromolecules* **2008**, *41*, 788–795.
- (20) Arcella, V.; Colaianna, P.; Maccone, P.; Sanguineti, A.; Gordano, A.; Clarizia, G.; Drioli, E. A study on a perfluoropolymer purification and its application to membrane formation. *J. Membr. Sci.* **1999**, *163*, 203–209.
- (21) Prabhakar, R. S.; Freeman, B. D.; Roman, I. Gas and Vapor sorption and permeation in poly(2,2,4-trifluoromethoxy-1,3-dioxole-co-tetrafluoroethylene). *Macromolecules* **2004**, *37*, 7688–7697.
- (22) Robeson, L. B. The upper bound revisited. *J. Membr. Sci.* **2008**, *320*, 390–400.
- (23) Hu, C.-C.; Chang, C.-S.; Ruaan, R.-C.; Lai, J.-Y. Effect of free volume and sorption on membrane gas transport. *J. Membr. Sci.* **2003**, *226*, 51–61.
- (24) Gardlund, Z. G. Effect of a polymer matrix on photochromism of some benzospirans. *J. Polym. Sci., Polym. Lett. Ed.* **1968**, *B6*, 57–61.
- (25) Mita, I.; Horie, K.; Hirao, K. Photochemistry in polymer solids. 9. Photoisomerization of azobenzene in a polycarbonate film. *Macromolecules* **1989**, *22*, 558–563.
- (26) Scot Royal, J.; Torkelson, J. M. Photochromic and fluorescent probe studies in glassy polymer matrices. 5. Effects of physical aging on bisphenol-A polycarbonate and poly(vinyl acetate) as sensed by a size distribution of photochromic probes. *Macromolecules* **1992**, *25*, 4792–4796.
- (27) Sung, C. S. P.; Gould, I. R.; Turro, N. J. Pulsed laser spectroscopic study of the photoisomerization of azo labels at three different locations on a polystyrene chain. *Macromolecules* **1984**, *17*, 1447–1451.
- (28) Scot Royal, J.; Victor, J. G.; Torkelson, J. M. Photochromic and fluorescent probe studies in glassy polymer matrices. 4. Effects of physical aging on poly(methyl methacrylate) as sensed by a size distribution of photochromic probes. *Macromolecules* **1992**, *25*, 729–734.
- (29) Ueda, M.; Kim, H. B.; Ikeda, T.; Ichimura, K. Photoisomerization of an azobenzene in sol-gel glass-films. *Chem. Mater.* **1992**, *4*, 1229–1233.
- (30) Ueda, M.; Kim, H. B.; Ikeda, T.; Ichimura, K. Photoisomerizability of an azobenzene covalently attached to silica-gel matrix. *J. Non-Cryst. Solids* **1993**, *163*, 125–132.
- (31) Algiers, J.; Sperr, P.; Egger, W.; Liszkay, L.; Kögel, G.; de Baerdemaeker, J.; Maurer, F. H. J. Free volume determination of azobenzene-PMMA copolymer by a pulsed low-energy positron lifetime beam with in-situ UV illumination. *Macromolecules* **2004**, *37*, 8035–8042.
- (32) Serra, F.; Terentjev, E. M. Effect of solvent viscosity and polarity on the isomerisation of azobenzene. *Macromolecules* **2008**, *41*, 981–986.
- (33) Evans, R. A.; Hanley, T. L.; Skidmore, M. A.; Davis, T. P.; Such, G. K.; Yee, L. H.; Ball, G. E.; Lewis, D. A. The generic enhancement of photochromic dye switching speeds in a rigid polymer matrix. *Nat. Mater.* **2005**, *4*, 249–253.
- (34) Ellison, C. J.; Torkelson, J. M. The distribution of glass-transition temperatures in nanoscopically confined glass formers. *Nat. Mater.* **2003**, *2*, 695–700.
- (35) Ellison, C. J.; Torkelson, J. M. Sensing the Glass Transition in Thin and Ultrathin Polymer Films via Fluorescence Probes and Labels. *J. Polym. Sci., Part B: Polym. Phys.* **2002**, *40*, 2745–2758.
- (36) Bartos, J. Positron Annihilation Spectroscopy of Polymers and Rubbers. In *Encyclopedia of Analytical Chemistry*; Meyers, R. A., Ed.; Wiley: Chichester, UK, 2000; p 7968.
- (37) Kobayashi, Y.; Zheng, W.; Meyer, E. F.; McGervey, J. D.; Jamieson, A. M.; Simha, R. Free volume and physical aging of poly(vinyl acetate) studied by positron annihilation. *Macromolecules* **1989**, *22*, 2302–2306.
- (38) Hristow, H. A.; Bolan, B.; Yee, A. F.; Xie, L.; Gidley, D. W. Measurement of Hole Volume in Amorphous Polymers Using Positron Spectroscopy. *Macromolecules* **1996**, *29*, 8507–8516.
- (39) Shantarovich, V. P. Positron Annihilation and Free Volume Studies in Polymer Glasses. *J. Polym. Sci., Part B: Polym. Phys.* **2008**, *46*, 2485.
- (40) Tao, J. Positronium Annihilation in Molecular Substances. *J. Chem. Phys.* **1972**, *56*, 5499–5510.
- (41) Eldrup, M.; Lightbody, D.; Sherwood, J. N. The temperature dependence of positron lifetimes in solid pivalic acid. *Chem. Phys.* **1981**, *63*, 51–58.
- (42) Jean, Y. C. Positron annihilation spectroscopy for chemical analysis: A novel probe for microstructural analysis of polymers. *Microchem. J.* **1990**, *42*, 72–102.
- (43) Jasinska, B.; Koziel, A. E.; Goworek, T. Ortho-positronium lifetimes in nonspherical voids. *J. Radioanal. Nucl. Chem.* **1996**, *210*, 617.
- (44) Mokrushin, A. D.; Tatur, A. O.; Shantarovich, V. P. Reactions of positronium atoms with O₂ in silicagel pores. *Izv. Acad. Nauk SSSR, Ser. Khim.* **1973**, *6*, 1216.
- (45) Consolati, G.; Genco, I.; Pegoraro, M.; Zanderighi, L. Positron annihilation lifetime in polytrimethylsilylpropyne: free volume determination and time dependence of permeability. *J. Polym. Sci., Part B: Polym. Phys.* **1996**, *34*, 357.
- (46) Shantarovich, V. P.; Kevdina, I. B.; Yampolskii, Yu. P.; Alentiev, A. Yu. Positron Annihilation Lifetime Study of High and Low Free Volume Glassy Polymers: Effects of Free Volume Sizes on the Permeability and Permselectivity. *Macromolecules* **2000**, *33*, 7453–7466.
- (47) Braun, J.-M.; Guillet, J. E. Study of polymers by inverse gas chromatography. *Adv. Polym. Sci.* **1976**, *21*, 107–145.
- (48) Theodorou, D. N. Principles of molecular simulation of gas transport in polymers. In *Materials Science of Membranes for Gas and Vapor Separation*; Yampolskii, Yu., Pinna, I., Freeman, B. D., Eds.; John Wiley & Sons: Chichester, England, 2006; Chapter 2, pp 49–94.
- (49) Hofmann, D.; Entrialgo-Castano, M.; Lebret, A.; Heuchel, M.; Yampolskii, Yu. Molecular modeling investigation of free volume distributions in stiff chain polymers with conventional and ultra-high free volume: comparison between molecular modeling and positron lifetime studies. *Macromolecules* **2003**, *36*, 8528–8538.
- (50) Wang, X.; Raharjo, R. D.; Lee, H. J.; Freeman, B. D.; Sanchez, I. C. Molecular Simulation and Experimental Study of Substituted Polyacetylenes: Fractional Free Volume, Cavity Size Distribution and Diffusion Coefficients. *J. Phys. Chem. B* **2006**, *110*, 12666–12672.
- (51) Heuchel, M.; Hofmann, D.; Pullumbi, P. Molecular modeling of small molecule permeation in polyimides and its correlation to free volume distributions. *Macromolecules* **2004**, *37*, 201–214.
- (52) Macchione, M.; Jansen, J. C.; De Luca, G.; Tocci, E.; Longeri, M.; Drioli, E. Experimental analysis and simulation of the gas transport in dense Hyflon® AD60X membranes. Influence of residual solvent. *Polymer* **2007**, *48*, 2619–2635.
- (53) Jansen, J. C.; Macchione, M.; Drioli, E. High flux asymmetric gas separation membranes of modified poly(ether ether ketone) prepared by the dry phase inversion technique. *J. Membr. Sci.* **2005**, *255*, 167–180.

- (54) Fischer, E. The Calculation of Photostationary States in Systems A \rightleftharpoons B When Only A Is Known. *J. Phys. Chem.* **1967**, *71*, 3704–3706.
- (55) Blanc, J.; Ross, D. L. A procedure for determining the absorption spectra of mixed photochromic isomers not requiring their separation. *J. Phys. Chem.* **1968**, *72*, 2817–2824.
- (56) Jean, Y. C., Mallon, P. E., Schrader, D. M., Eds. *Principles and Applications of Positron and Positronium Chemistry*; World Scientific: Singapore, 2003.
- (57) Shantarovich, V. Positronium atom in solids - peculiarities of formation and interaction with free volume nanostructure. *J. Nucl. Radiochem. Sci.* **2006**, *7*, 37–52.
- (58) Reid, R. C.; Sherwood, T. K. *The Properties of Gases and Liquids*; McGraw-Hill: New York, 1966.
- (59) Arcella, V.; Brinati, G.; Colaianna, P.; Sanguineti, A.; Gordano, A.; Clarizia, G.; Molinari, R.; Drioli, E. Proceedings of Ravello Conference “New Frontiers for Catalytic Membrane Reactors and Other Membrane Processes”, **1999**, p 102.
- (60) Jansen, J. C.; Friess, K.; Drioli, E., manuscript in preparation.
- (61) (a) Theodorou, D. N.; Suter, U. W. Detailed molecular structure of a vinyl polymer glass. *Macromolecules* **1985**, *18*, 1467–1478. (b) Theodorou, D. N.; Suter, U. W. Atomistic modeling of mechanical properties of polymeric glasses. *Macromolecules* **1986**, *19*, 139–154.
- (62) *Polymer User Guide, Amorphous Cell Section, Version 4.0.0*; Molecular Simulations Inc.: San Diego, CA, 1999.
- (63) (a) Sun, H.; Rigby, D. Polysiloxanes: Ab Initio Forcefield and Structural, Conformational and Thermophysical Properties. *Spectrochim. Acta, Part A* **1997**, *53*, 1301. (b) Rigby, D.; Sun, H.; Eichinger, B. E. Computer Simulations of Poly(ethylene oxide): Forcefield, PVT Diagram and Cyclization Behavior. *Polym. Int.* **1997**, *44*, 311.
- (64) Hofmann, D.; Fritz, L.; Ulbrich, J.; Schepers, C.; Böehning, M. Detailed atomistic molecular modeling of small molecule diffusion and solution processes in polymeric membrane materials. *Macromol. Theory Simul.* **2000**, *9*, 293–327.
- (65) Tocci, E.; Pullumbi, P. Molecular simulation of realistic membrane models of alkylated PEEK membranes. *Mol. Simul.* **2006**, *32*, 145–154.
- (66) Jansen, J. C.; Macchione, M.; Drioli, E. On the unusual solvent retention and the effect on the gas transport in perfluorinated Hyflon AD® membranes. *J. Membr. Sci.* **2007**, *287*, 132–137.
- (67) *Material Studio Software Package*; Accelrys Inc.: San Diego, CA, 2004.
- (68) Gee, R. H.; Fried, L. E.; Cook, R. C. Structure of Chlorotrifluoroethylene/Vinylidene Fluoride Random Copolymers and Homopolymers by Molecular Dynamics Simulations. *Macromolecules* **2001**, *34*, 3050–3059.
- (69) Hofmann, D.; Heuchel, M.; Yampolskii, Yu.; Khotimskii, V.; Shantarovich, V. Free volume distribution in ultrahigh and lower free volume polymers: comparison between molecular modeling and positron lifetime studies. *Macromolecules* **2002**, *35*, 2129–2140.
- (70) Andrea, T. A.; Swope, W. C.; Andersen, H. C. The role of long range forces in determining the structure and properties of liquid water. *J. Chem. Phys.* **1983**, *79*, 4576–4584.
- (71) Berendsen, H. J. C.; Postma, J. P. M.; Van Gunsteren, W. F.; DiNola, A.; Haak, J. R. Molecular dynamics with coupling to an external bath. *J. Chem. Phys.* **1984**, *81*, 3684.
- (72) *InsightII 4.0.0.P+, Polymerizer, Discover, Amorphous Cell, Builder, Sorption Modules 2001*; Accelrys Inc.: San Diego, CA, 2001.
- (73) Bondi, A. Van der Waals Volumes and Radii. *J. Phys. Chem.* **1964**, *68*, 441–451.
- (74) Höck, O.; Böhnning, M.; Heuchel, M.; Hofmann, D. Detailed Atomistic Simulation of Gas Sorption Isotherms in Swelling Glassy Polymers, *J. Membr. Sci.*, in preparation.
- (75) The cis fraction in solution was not available in the literature for 4,4-dinitrostilbene, and therefore a value of 85% was assumed for the isomerization efficiency in dilute solution. This is about the average value of various different probes reported in the literature, most of them lying in the range from about 80% to 90% (Table 1 of the Supporting Information and ref 16).
- (76) Takeuchi, S.; Ruhman, S.; Tsuneda, T.; Chiba, M.; Taketsugu, T.; Tahara, T. Spectroscopic Tracking of Structural Evolution in Ultrafast Stilbene Photoisomerization. *Science* **2008**, *322*, 1073–1077.
- (77) Traetteberg, M.; Hilmo, I.; Hagen, K. A gas electron diffraction study of the molecular structure of trans-azobenzene. *J. Mol. Struct.* **1977**, *39*, 231–239.
- (78) Orlandi, G.; Siebrand, W. Model for the direct photo-isomerization of stilbene. *Chem. Phys. Lett.* **1975**, *30*, 352–354.
- (79) Birks, J. B. The photo-isomerization of stilbene. *Chem. Phys. Lett.* **1976**, *38*, 437–440.
- (80) Shantarovich, V. P.; Suzuki, T.; Ito, Y.; Kondo, K.; Yu, R. S.; Budd, P. M.; Yampolskii, Yu.P.; Berdonosov, S. S.; Eliseev, A. A. Structural heterogeneity in glassy polymer materials revealed by positron annihilation and other supplementary techniques. *Phys. Status Solidi C* **2007**, *4*, 3776–3779.
- (81) Shantarovich, V. P.; Suzuki, T.; He, C.; Davankov, V. A.; Pastukhov, A. V.; Tsyurupa, M. P.; Kondo, K.; Ito, Y. Positron annihilation study of hyper-cross-linked polystyrene networks. *Macromolecules* **2002**, *35*, 9723–9729.
- (82) Kirkegaard, P.; Pederson, N. J.; Eldrup, M. *PATFIT-88: A data processing system for positron annihilation spectra on mainframe and personal computers, Risoe-M-2740*; Risoe National Laboratory DK-4000: Roskilde, Denmark, Feb 1989.
- (83) Alemtov, A. Yu.; Shantarovich, A. V. P.; Merkel, T. C.; Bondar, V. I.; Freeman, B. D.; Yampolskii, Yu.P. Gas and Vapor Sorption, Permeation, and Diffusion in Glassy Amorphous Teflon AF1600. *Macromolecules* **2002**, *35*, 9513–9522.
- (84) (a) Dlubek, G.; Hübner, Ch.; Eichler, S. Do the CONTIN or the MELT programs accurately reveal the o-Ps lifetime distribution in polymers? Analysis of experimental lifetime spectra of amorphous polymers. *Nucl. Instrum. Methods Phys. Res., Sect. B* **1998**, *142*, 191–202. (b) Dlubek, G.; Eichler, S. Do MELT or CONTIN Programs Accurately Reveal the o-Ps Lifetime Distribution in Polymers? Analysis of Simulated Lifetime Spectra. *Phys. Status Solidi* **1998**, *168*, 333–350.
- (85) Dlubek, G.; Saarinen, K.; Fretwell, H. M. Positron states in polyethylene and polytetrafluoroethylene: A positron lifetime and Doppler-broadening study. *Nucl. Instrum. Methods Phys. Res., Sect. B* **1998**, *142*, 139–155.
- (86) Liu, J.; Jean, Y. C.; Yang, H. Free-Volume Hole Properties of Polymer Blends Probed by Positron Annihilation Spectroscopy: Miscibility. *Macromolecules* **1995**, *28*, 5774–5779.
- (87) Yampolskii, Yu.; Berezkin, V.; Popova, T.; Korikov, A.; Freeman, B. D.; Bondar, V.; Merkel, T. C. Thermodynamics of sorption of gases and vapors by amorphous Teflons AF. *Polym. Sci. A* **2000**, *42*, 679–688.
- (88) Yampolskii, Yu.; Soloviev, S.; Gringolts, M. Thermodynamics of sorption and free volume of poly(5,6-bis(trimethylsilyl)norbornene). *Polymer* **2004**, *45*, 6945–6952.
- (89) Tocci, E.; Hofmann, D.; Paul, D.; Russo, N.; Drioli, E. A molecular simulation study on gas diffusion in a dense poly(ether-ether-ketone) membrane. *Polymer* **2001**, *42*, 521–533.
- (90) Willmore, F. T.; Wang, X.; Sanchez, I. C. Free volume properties of model fluids and polymers: shape and connectivity. *J. Polym. Sci., Part B: Polym. Phys.* **2006**, *44*, 1385–1393.